Uncertainty principles for inverse source problems for electromagnetic and elastic waves

Roland Griesmaier[1] **and John Sylvester**[2]

[1] Institut für Mathematik, Universität Würzburg, 97074 Würzburg, Germany
[2] University of Washington, Seattle, Washington 98195, U.S.A.

E-mail: roland.griesmaier@uni-wuerzburg.de, sylvest@uw.edu

Last modified: 15 February 2018

Abstract. In isotropic homogeneous media, far fields of time-harmonic electromagnetic waves radiated by compactly supported volume currents, and elastic waves radiated by compactly supported body force densities can be modelled in very similar fashion. Both are projected restricted Fourier transforms of vector-valued source terms. In this work we generalize two types of uncertainty principles recently developed for far fields of scalar-valued time-harmonic waves in [R. Griesmaier and J. Sylvester, *SIAM J. Appl. Math.* 77 (2017)] to this vector-valued setting. These uncertainty principles yield stability criteria and algorithms for splitting far fields radiated by collections of well-separated sources into the far fields radiated by individual source components, and for the restoration of missing data segments. We discuss proper regularization strategies for these inverse problems, provide stability estimates based on the new uncertainty principles, and comment on reconstruction schemes. A numerical example illustrates our theoretical findings.

Keywords: Inverse source problem, Maxwell's equations, Navier equations, uncertainty principles, far field splitting, data completion, stability estimates

Mathematics subject classifications (MSC2010): 35R30, (65N21)

1. Introduction

We continue our previous investigations of uncertainty principles for far fields of time-harmonic waves in unbounded homogeneous isotropic media as a means to provide criteria, stability estimates and reconstruction algorithms for inverse source problems with compactly supported sources in homogeneous isotropic media. So far these uncertainty principles have been established for time-harmonic scalar waves, i.e., for solutions to the scalar Helmholtz equation in [7, 8]. Here we extend these results to vector-valued electromagnetic and elastic waves described by Maxwell's equations and the Navier system. In both cases the far field of a wave radiated by a compactly supported source distribution coincides up to a constant with the tangential components (for electromagnetic waves and elastic shear waves) or with the normal components (for

elastic pressure waves) of the Fourier transform of a vector-valued source term restricted to a sphere.

Although it is in general not possible to uniquely recover a source from such projected restricted Fourier transforms, it is possible to recover information about its support [10, 17, 18, 23, 26]. In particular, unique continuation of solutions to the homogeneous Maxwell's equations and the Navier system tell us that no two sources with disjoint support can radiate exactly the same far fields. Accordingly, the subspaces of far fields radiated from disjoint compact sets intersect only at the origin, and therefore the *far field splitting problem*, to decompose a far field radiated by an ensemble of compactly supported sources with disjoint supports into a sum of far fields, each of which is radiated by an individual source component, has a unique solution. Similarly, the analyticity of Fourier transforms of compactly supported functions tells us that the far field radiated by a compactly supported source cannot vanish on an open subset of the sphere, so that the subspace of far fields radiated from a compact set and the subspace of vector fields vanishing on an open subset of the sphere intersect only at the origin. Therefore the *data completion problem*, to recover a far field radiated by a compactly supported source on the entire sphere from observations on an open subset of the sphere, has a unique solution. It is, however, well known that without further assumptions both inverse problems are severely ill-posed.

In this work we extend a regularization strategy, corresponding stability estimates, and reconstruction algorithms for these inverse problems that have recently been developed for the scalar case in [7, 8] to the vector-valued setting. We calculate the singular value decompositions of the projections (onto tangential and normal components) of restricted Fourier transforms. These operators map L^2-sources supported in a ball to their radiated far fields. We first characterize the subspaces of *nonevanescent far fields*. These are subspaces of far fields that can be radiated by a limited power source, and at the same time have enough energy to be detected by a receiver with limited sensitivity. It is a characteristic of wave propagation that these subspaces depend very weakly on the power of the source and the sensitivity of the receiver. We call this characterization a *regularized Picard criterion*, and our regularization strategy is to recover only the nonevanescent part of the far fields, neglecting the evanescent part, which is very small for all practically relevant far fields.

We prove two uncertainty principles for nonevanescent far fields. The *uncertainty principle for far field translation* gives a lower bound on the angle between nonevanescent far fields radiated from disjoint balls, which immediately implies an upper bound on the condition number of the far field splitting problem for the nonevanescent parts of the far fields. The bound depends simply on three physical parameters, the wave number, the diameters of the balls, and the distances between them. Similarly, the *uncertainty principle for data completion* gives a lower bound on the angle between nonevanescent far fields radiated from a ball and vector fields vanishing on an open subset Ω of the sphere, which in turn implies an upper bound on the condition number of the data completion problem, where we reconstruct the nonevanescent part of the far field on Ω.

In this case the bound depends on the wave number, the diameter of the ball, and the area of Ω.

Although the calculations are a bit more difficult, the basic structure of these results, as well as their proofs, are similar to the three-dimensional scalar case, with the spherical harmonic decomposition of a function replaced by the decomposition of a vector field into vector spherical harmonics. There are, however, some unexpected differences. Half of the singular values of the tangential restricted Fourier transform, which maps sources to far fields of electromagnetic waves and elastic shear waves, exactly coincide with the singular values of the corresponding operator in the three-dimensional scalar case, but the other half, and the singular values of the normal restricted Fourier transform, which maps sources to far fields of elastic pressure waves, differ. While the criterion itself changes, the qualitative properties of the singular values used to justify the regularized Picard criterion turn out to be comparable to the scalar case, so the proof is analogous. Furthermore, the analysis of the uncertainty principles in the vector-valued case using vector spherical harmonics instead of scalar spherical harmonics requires some subtle modifications of the previous arguments.

On the other hand, once the uncertainty principles have been established, it is relatively straightforward to carry over the stability results from [7, 8] and the numerical algorithms from [5, 6] to the vector-valued setting. Therefore, we only state three basic stability estimates and describe one numerical algorithm in detail, referring the reader to [5, 6, 7, 8] for proofs, and for further results and algorithms.

Alternate approaches to far field splitting that however, so far, lack a rigorous stability analysis have been published in [12, 22] (see also [9] for a method to separate time-dependent wave fields due to multiple sources).

The outline of this paper is as follows. After introducing some notation in the next section, we provide the theoretical background for the time-harmonic electromagnetic and elastic source problems in Section 3. In Section 4 we derive the singular value decompositions of the tangential and normal restricted far field operators and we discuss the regularized Picard criterion to characterize nonevanescent far fields. In Section 5 we develop the uncertainty principles for far field translation and for the vector spherical harmonic expansion of vector fields on the sphere. We briefly comment on applications of these uncertainty principles in stability estimates for least squares algorithms for far field splitting and data completion in Section 6. In Section 7 we provide a numerical example.

2. Preliminaries

We start by introducing some notation that we will use throughout this article. The boldface Latin letters $\boldsymbol{x}, \boldsymbol{y}, \boldsymbol{c}$ always refer to space variables in $\mathbb{R}^3$, $\boldsymbol{x} \cdot \boldsymbol{y}$ and $\boldsymbol{x} \times \boldsymbol{y}$ denote the scalar product and the vector product of $\boldsymbol{x}$ and $\boldsymbol{y}$, and $|\boldsymbol{x}|$ is the Euclidean norm of $\boldsymbol{x}$.

The variable on the unit sphere $S^2 \subseteq \mathbb{R}^3$ will typically be denoted by $\boldsymbol{\theta}$, unless

it has been derived from a space variable by normalization, in which case the variable inherits the name of the space variable augmented by a hat symbol, e.g., $\widehat{\boldsymbol{x}} := \boldsymbol{x}/|\boldsymbol{x}|$. The unit outward normal vector field on S^2 is denoted by $\boldsymbol{\nu}$ and satisfies $\boldsymbol{\nu}(\boldsymbol{\theta}) = \boldsymbol{\theta}$ for all $\boldsymbol{\theta} \in S^2$.

For each fixed $\boldsymbol{\theta} \in S^2$ we denote by $\boldsymbol{\theta}^\perp$ the subspace of $\mathbb{R}^3$ perpendicular to $\boldsymbol{\theta}$ (i.e., the tangent space to the unit sphere at $\boldsymbol{\theta}$), and we write $\Pi_{\boldsymbol{\theta}^\perp}$ and $\Pi_{\boldsymbol{\theta}}$ for the orthogonal projections onto $\boldsymbol{\theta}^\perp$ and $\boldsymbol{\theta}$, respectively, i.e., $\Pi_{\boldsymbol{\theta}^\perp}\boldsymbol{x} := -\boldsymbol{\theta} \times (\boldsymbol{\theta} \times \boldsymbol{x})$ and $\Pi_{\boldsymbol{\theta}}\boldsymbol{x} := (\boldsymbol{\theta} \cdot \boldsymbol{x})\boldsymbol{\theta}$. The spaces of tangential and normal p-integrable vector fields on the sphere are given, for $1 \leq p \leq \infty$, by

$$\begin{aligned} L_t^p(S^2, \mathbb{C}^3) &:= \{\boldsymbol{u} \in L^p(S^2, \mathbb{C}^3) \mid \boldsymbol{\nu} \cdot \boldsymbol{u} = 0 \ \text{ a.e. on } S^2\}, \\ L_n^p(S^2, \mathbb{C}^3) &:= \{\boldsymbol{u} \in L^p(S^2, \mathbb{C}^3) \mid \boldsymbol{\nu} \times \boldsymbol{u} = 0 \ \text{ a.e. on } S^2\}, \end{aligned}$$

with the standard $L^p(S^2, \mathbb{C}^3)$-norm. We sometimes consider the orthogonal projections $\Pi_{\boldsymbol{\theta}}$ and $\Pi_{\boldsymbol{\theta}^\perp}$ as a function of $\boldsymbol{\theta}$, i.e., as operators

$$\begin{aligned} \Pi_t &: L^2(S^2, \mathbb{C}^3) \to L_t^2(S^2, \mathbb{C}^3), \quad (\Pi_t \boldsymbol{u})(\boldsymbol{\theta}) := \Pi_{\boldsymbol{\theta}^\perp} \boldsymbol{u}(\boldsymbol{\theta}), \\ \Pi_n &: L^2(S^2, \mathbb{C}^3) \to L_n^2(S^2, \mathbb{C}^3), \quad (\Pi_n \boldsymbol{u})(\boldsymbol{\theta}) := \Pi_{\boldsymbol{\theta}} \boldsymbol{u}(\boldsymbol{\theta}). \end{aligned}$$

For smooth functions on S^2 the *surface gradient* **Grad** and the *surface vector curl* **Curl** may be defined in the usual way via parametric representation (cf., e.g., [14, pp. 326–331]). If $P \in C^1(\mathbb{R}^3, \mathbb{C})$ and its restriction to S^2 is $p \in C^1(S^2, \mathbb{C})$, then

$$\nabla P = \frac{\partial P}{\partial \boldsymbol{\nu}} \boldsymbol{\nu} + \mathbf{Grad}\, p \qquad \text{and} \qquad \mathbf{Curl}\, p = -\boldsymbol{\nu} \times \nabla P.$$

The dual operators of $-\mathbf{Grad}$ and **Curl** (with respect to the duality pairing given by the L^2 bilinear forms) are the *surface divergence* Div and the *surface scalar curl* Curl, i.e., for any $p \in C^1(S^2, \mathbb{C})$ and $\boldsymbol{u} \in C^1(S^2, \mathbb{C}^3)$,

$$\int_{S^2} p \operatorname{Div} \boldsymbol{u} \, \mathrm{d}s = -\int_{S^2} \boldsymbol{u} \cdot \mathbf{Grad}\, p \, \mathrm{d}s \quad \text{and} \quad \int_{S^2} p \operatorname{Curl} \boldsymbol{u} \, \mathrm{d}s = \int_{S^2} \boldsymbol{u} \cdot \mathbf{Curl}\, p \, \mathrm{d}s. \tag{3}$$

Throughout we let scalar operators act on vectors componentwise and vector operators on matrices column by column.

3. Far fields radiated by compactly supported sources

We begin with a brief discussion of the direct source problems for time-harmonic electromagnetic and elastic waves with compactly supported volume current and body force densities at a fixed *frequency* $\omega > 0$. Before we introduce each problem individually in the next two subsections, we give a simple lemma to explain why we will consider the far fields of solutions to both model equations in a unified framework. The lemma below indicates how the solutions to both the Maxwell's equations of electromagnetics and the Navier equations of linear elasticity can be calculated from the solutions to the vector Helmholtz equation.

The vector Laplacian on $\mathbb{R}^3$ is defined as $\Delta := -\mathbf{curl}\,\mathbf{curl} + \nabla\,\mathrm{div}$ and it is convenient to write the vector Helmholtz equation as

$$\frac{1}{k^2}\,\Delta \boldsymbol{U} + \boldsymbol{U} \;=\; -\boldsymbol{F}\,,$$

where $\boldsymbol{U}$ and $\boldsymbol{F}$ are vector-valued functions or distributions on $\mathbb{R}^3$.

Lemma 3.1. *Suppose that a and b are real constants and that $\boldsymbol{U}$, $\boldsymbol{V}$, and $\boldsymbol{F}$ satisfy*

$$a^2\Delta \boldsymbol{U} + \boldsymbol{U} \;=\; -\boldsymbol{F} \qquad \text{and} \qquad b^2\Delta \boldsymbol{V} + \boldsymbol{V} \;=\; -\boldsymbol{F}\,. \tag{4}$$

Then $\boldsymbol{W}$, defined by any of the three (equal) formulas below,

$$\boldsymbol{W} \;:=\; \begin{cases} \boldsymbol{U} + \nabla\,\mathrm{div}(a^2\boldsymbol{U} - b^2\boldsymbol{V})\,, & \text{(5a)} \\ \boldsymbol{V} + \mathbf{curl}\,\mathbf{curl}(a^2\boldsymbol{U} - b^2\boldsymbol{V})\,, & \text{(5b)} \\ -\boldsymbol{F} + a^2\mathbf{curl}\,\mathbf{curl}\boldsymbol{U} - b^2\nabla\,\mathrm{div}\,\boldsymbol{V}\,, & \text{(5c)} \end{cases}$$

satisfies

$$\left(-a^2\mathbf{curl}\,\mathbf{curl} + b^2\nabla\,\mathrm{div} + 1\right)\boldsymbol{W} \;=\; -\boldsymbol{F}\,. \tag{6}$$

Proof. We rewrite (4) as

$$a^2\nabla\,\mathrm{div}\,\boldsymbol{U} \;=\; -\boldsymbol{F} + a^2\mathbf{curl}\,\mathbf{curl}\,\boldsymbol{U} - \boldsymbol{U}\,, \tag{7a}$$

$$b^2\nabla\,\mathrm{div}\,\boldsymbol{V} \;=\; -\boldsymbol{F} + b^2\mathbf{curl}\,\mathbf{curl}\,\boldsymbol{V} - \boldsymbol{V}\,. \tag{7b}$$

Substituting the right hand side of (7a) into (5a) gives (5c), and substituting (7b) into (5c) gives (5b).

To verify (6), we utilize (5a) and (5b) to write

$$-a^2\mathbf{curl}\,\mathbf{curl}\,\boldsymbol{W} \;=\; -a^2\mathbf{curl}\,\mathbf{curl}\,\boldsymbol{U} \qquad \text{and} \qquad b^2\nabla\,\mathrm{div}\;\boldsymbol{W} \;=\; b^2\nabla\,\mathrm{div}\,\boldsymbol{V}\,,$$

add these to (5a), and use (4) to obtain

$$\left(-a^2\mathbf{curl}\,\mathbf{curl} + b^2\nabla\,\mathrm{div}\right)\boldsymbol{W} + \boldsymbol{W} \;=\; a^2\Delta\boldsymbol{U} + \boldsymbol{U} \;=\; -\boldsymbol{F}\,.$$

□

If $\boldsymbol{U}$ and $\boldsymbol{V}$ are the unique radiating solutions of the vector Helmholtz equations (4) given by the volume potential

$$k^2\int_{\mathbb{R}^3} \Phi_k(\boldsymbol{x}-\boldsymbol{y})\boldsymbol{F}(\boldsymbol{y})\;\mathrm{d}\boldsymbol{y}\,, \tag{8}$$

where Φ_k denotes the fundamental solution for the three-dimensional scalar Helmholtz equation,

$$\Phi_k(\boldsymbol{x}) \;:=\; \frac{1}{4\pi}\,\frac{e^{\mathrm{i}k|\boldsymbol{x}|}}{|\boldsymbol{x}|}\,, \qquad \boldsymbol{x}\in\mathbb{R}^3\setminus\{0\}\,, \tag{9}$$

and $k^2 = 1/a^2$ and $k^2 = 1/b^2$ for $\boldsymbol{U}$ and $\boldsymbol{V}$, respectively, then $\boldsymbol{W}$ is also radiating. The radiation conditions will be described in more detail in the next two subsections.

In the case that $a^2 = 1/k^2$, $b^2 = 0$, and $\boldsymbol{F} = \boldsymbol{J}$, the equation (6) reduces to the second order Maxwell's equations for the electric field in (10) below. If instead we choose $a^2 = \mu/\omega^2$ and $b^2 = (\lambda+2\mu)/\omega^2$ we obtain the Navier system in (15).

3.1. Electromagnetic waves

We consider a homogeneous and isotropic medium with constant *electric permittivity* $\varepsilon > 0$ and constant *magnetic permeability* $\mu > 0$. Accordingly, the associated *wave number* is $k := \omega\sqrt{\varepsilon\mu}$.

Given a compactly supported *volume current density* $\boldsymbol{J} \in L^2_0(\mathbb{R}^3, \mathbb{C}^3)$, the electromagnetic wave radiated by $\boldsymbol{J}$ and described by the *electric field* $\boldsymbol{E}$ satisfies the second order Maxwell system

$$\mathbf{curl}\,\mathbf{curl}\boldsymbol{E} - k^2\boldsymbol{E} \;=\; k^2\boldsymbol{J} \qquad \text{in } \mathbb{R}^3 \tag{10a}$$

and the Silver-Müller radiation condition

$$\lim_{|\boldsymbol{x}|\to\infty} |\boldsymbol{x}|((\mathbf{curl}\boldsymbol{E}) \times \widehat{\boldsymbol{x}} - \mathrm{i}k\boldsymbol{E}) \;=\; 0\,. \tag{10b}$$

The mapping properties of the volume potential (8) and (5a) (with $a^2 = 1/k^2$ and $b^2 = 0$) show that the unique solution to (10) satisfies $\boldsymbol{E} \in H_{\mathrm{loc}}(\mathbf{curl}, \mathbb{R}^3)$, and (5c) (with $\boldsymbol{F} = \boldsymbol{J}$) yields

$$\boldsymbol{E}(\boldsymbol{x}) \;=\; -\boldsymbol{J}(\boldsymbol{x}) + \mathbf{curl}\,\mathbf{curl}\int_{\mathbb{R}^3} \Phi_k(\boldsymbol{x}-\boldsymbol{y})\boldsymbol{J}(\boldsymbol{y})\,\mathrm{d}\boldsymbol{y}\,, \qquad \boldsymbol{x} \in \mathbb{R}^3\,,$$

(see also, [13, Thm. 3.1]). As usual, $H_{\mathrm{loc}}(\mathbf{curl}, \mathbb{R}^3)$ denotes the space of locally square integrable vector fields with locally square integrable curl.

After rescaling $\boldsymbol{E}(\boldsymbol{x}) = \boldsymbol{E}(k\boldsymbol{x})$ and $\boldsymbol{J}(\boldsymbol{x}) = \boldsymbol{J}(k\boldsymbol{x})$, i.e., measuring distances in wavelengths,[1] we may assume in our calculations below that $k = 1$. Accordingly,

$$\boldsymbol{E}(\boldsymbol{x}) \;=\; -\boldsymbol{J}(\boldsymbol{x}) + \mathbf{curl}\,\mathbf{curl}\int_{\mathbb{R}^3} \Phi(\boldsymbol{x}-\boldsymbol{y})\boldsymbol{J}(\boldsymbol{y})\,\mathrm{d}\boldsymbol{y}\,, \qquad \boldsymbol{x} \in \mathbb{R}^3\,, \tag{11}$$

where Φ denotes the fundamental solution from (9) with $k = 1$. We can restore the dependence on wavelength by simply rescaling the spatial variable (i.e., replacing all parameters with the same units as $\boldsymbol{x}$ by k times that quantity) when we are done.

The asymptotics of the fundamental solution,

$$\mathbf{curl}_x\,\mathbf{curl}_x(\Phi(\boldsymbol{x}-\boldsymbol{y})\boldsymbol{p}) \;=\; \frac{1}{4\pi}\frac{e^{\mathrm{i}|\boldsymbol{x}|}}{|\boldsymbol{x}|}\Big(e^{-\mathrm{i}\widehat{\boldsymbol{x}}\cdot\boldsymbol{y}}\Pi_{\widehat{\boldsymbol{x}}^\perp}\boldsymbol{p} + \mathcal{O}\Big(\frac{|\boldsymbol{p}|}{|\boldsymbol{x}|}\Big)\Big)\,, \quad \boldsymbol{p} \in \mathbb{C}^3\,,\ |\boldsymbol{x}| \to \infty\,, \tag{12}$$

(cf., e.g., [2, p. 199]) tell us that

$$\boldsymbol{E}(\boldsymbol{x}) \;=\; \frac{1}{4\pi}\frac{e^{\mathrm{i}|\boldsymbol{x}|}}{|\boldsymbol{x}|}\boldsymbol{A}(\widehat{\boldsymbol{x}}) + \mathcal{O}(|\boldsymbol{x}|^{-2}) \qquad \text{as } |\boldsymbol{x}| \to \infty\,,$$

where $\boldsymbol{A} \in L^2_t(S^2, \mathbb{C}^3)$, which is known as the *electric far field* radiated by $\boldsymbol{J}$. It is given by

$$\boldsymbol{A}(\boldsymbol{\theta}) \;=\; \Pi_{\boldsymbol{\theta}^\perp}\Big(\int_{\mathbb{R}^3} e^{-\mathrm{i}\boldsymbol{\theta}\cdot\boldsymbol{y}}\boldsymbol{J}(\boldsymbol{y})\,\mathrm{d}\boldsymbol{y}\Big)\,, \qquad \boldsymbol{\theta} \in S^2\,, \tag{13}$$

i.e., the vector field $\boldsymbol{A}$ is just the tangential component of the Fourier transform of the source $\boldsymbol{J}$ evaluated on the unit sphere S^2.

[1] One unit represents 2π wavelengths.

Accordingly, the *electric far field operator* $\mathcal{F}_{\text{electric}}$, which maps compactly supported volume current densities to their radiated electric far fields, is a *tangential projected restricted Fourier transform*,

$$\mathcal{F}_{\text{electric}} : L^2_0(\mathbb{R}^3, \mathbb{C}^3) \to L^2_t(S^2, \mathbb{C}^3)\,, \quad \mathcal{F}_{\text{electric}}\boldsymbol{J} := \Pi_t(\widehat{\boldsymbol{J}}|_{S^2})\,. \tag{14}$$

3.2. Elastic waves

We consider a homogeneous and isotropic medium with constant *Lamé coefficients* $\lambda, \mu \in \mathbb{R}$ such that $\mu > 0$ and $\lambda + 2\mu > 0$. Accordingly, the associated *transversal* and *longitudinal wave numbers* corresponding to shear and pressure waves are $k_s := \omega/\sqrt{\mu}$ and $k_p := \omega/\sqrt{\lambda + 2\mu}$.

Given a compactly supported *body force density* $\boldsymbol{F} \in L^2_0(\mathbb{R}^3, \mathbb{C}^3)$, the elastic wave radiated by $\boldsymbol{F}$ and described by the *displacement field* $\boldsymbol{U}$ satisfies the Navier system

$$-\mu\,\mathbf{curl}\,\mathbf{curl}\boldsymbol{U} + (\lambda + 2\mu)\nabla\,\mathrm{div}\,\boldsymbol{U} + \omega^2\boldsymbol{U} \;=\; -\omega^2\boldsymbol{F} \qquad \text{in } \mathbb{R}^3 \tag{15a}$$

and the Kupradze radiation conditions

$$\begin{aligned} \lim_{|\boldsymbol{x}|\to\infty} |\boldsymbol{x}|(\mathbf{curl}\,\mathbf{curl}\,\boldsymbol{U} \times \widehat{\boldsymbol{x}} - \mathrm{i}k_s\mathbf{curl}\,\boldsymbol{U}) \;&=\; 0\,, \\ \lim_{|\boldsymbol{x}|\to\infty} |\boldsymbol{x}|(\widehat{\boldsymbol{x}} \cdot \nabla\,\mathrm{div}\,\boldsymbol{U} - \mathrm{i}k_p\,\mathrm{div}\,\boldsymbol{U}) \;&=\; 0\,. \end{aligned} \tag{15b}$$

Employing Lemma 3.1 with $a^2 = \mu/\omega^2$ and $b^2 = (\lambda + 2\mu)/\omega^2$, we may write the solution as $\boldsymbol{U} = -\boldsymbol{F} + \boldsymbol{U}_s + \boldsymbol{U}_p$ with

$$\begin{aligned} \boldsymbol{U}_s(\boldsymbol{x}) \;&=\; \mathbf{curl}\,\mathbf{curl} \int_{\mathbb{R}^3} \Phi_{k_s}(\boldsymbol{x} - \boldsymbol{y})\boldsymbol{F}(\boldsymbol{y})\;\mathrm{d}\boldsymbol{y}\,, \qquad \boldsymbol{x} \in \mathbb{R}^3\,, \\ \boldsymbol{U}_p(\boldsymbol{x}) \;&=\; -\nabla\,\mathrm{div} \int_{\mathbb{R}^3} \Phi_{k_p}(\boldsymbol{x} - \boldsymbol{y})\boldsymbol{F}(\boldsymbol{y})\;\mathrm{d}\boldsymbol{y}\,, \qquad \boldsymbol{x} \in \mathbb{R}^3\,, \end{aligned}$$

where $k_s = 1/a$ and $k_p = 1/b$ (see also [11, p. 196]). As can be seen from (5), $\boldsymbol{U} \in H^1_{\text{loc}}(\mathbb{R}^3, \mathbb{C}^3)$, the space of locally square integrable vector fields with locally square integrable gradient.

In the following we consider the *transversal* and the *longitudinal components* $\boldsymbol{U}_s$ and $\boldsymbol{U}_p$ of the radiated wave, i.e., the *shear wave* and the *pressure wave*, separately. After rescaling $\boldsymbol{U}_s(\boldsymbol{x}) = \boldsymbol{U}_s(k_s\boldsymbol{x})$ and $\boldsymbol{F}(\boldsymbol{x}) = \boldsymbol{F}(k_s\boldsymbol{x})$, i.e., measuring distances in transversal wavelengths, we may assume in our calculations below that $k_s = 1$ and consider

$$\boldsymbol{U}_s(\boldsymbol{x}) \;=\; \mathbf{curl}\,\mathbf{curl} \int_{\mathbb{R}^3} \Phi(\boldsymbol{x} - \boldsymbol{y})\boldsymbol{F}(\boldsymbol{y})\;\mathrm{d}\boldsymbol{y}\,, \qquad \boldsymbol{x} \in \mathbb{R}^3\,,$$

where Φ again denotes the fundamental solution from (9) with $k = 1$. Similarly, we find for the longitudinal component $\boldsymbol{U}_p$ that, after rescaling $\boldsymbol{U}_p(\boldsymbol{x}) = \boldsymbol{U}_p(k_p\boldsymbol{x})$ and $\boldsymbol{F}(\boldsymbol{x}) = \boldsymbol{F}(k_p\boldsymbol{x})$, i.e., measuring distances in longitudinal wavelengths,

$$\boldsymbol{U}_p(\boldsymbol{x}) \;=\; -\nabla\,\mathrm{div} \int_{\mathbb{R}^3} \Phi(\boldsymbol{x} - \boldsymbol{y})\boldsymbol{F}(\boldsymbol{y})\;\mathrm{d}\boldsymbol{y}\,, \qquad \boldsymbol{x} \in \mathbb{R}^3\,. \tag{17}$$

It is important to note that the rescaling is different for the two components $\boldsymbol{U}_s$ and $\boldsymbol{U}_p$ of the displacement field $\boldsymbol{U}$. This is possible because, as we will see next, the far fields of the shear wave and of the pressure wave are independent of each other.

The asymptotics of the fundamental solution (12) and

$$\nabla_x \operatorname{div}_x(\Phi(\boldsymbol{x}-\boldsymbol{y})\boldsymbol{p}) \;=\; -\frac{1}{4\pi}\frac{e^{\mathrm{i}|\boldsymbol{x}|}}{|\boldsymbol{x}|}\Big(e^{-\mathrm{i}\widehat{\boldsymbol{x}}\cdot\boldsymbol{y}}\Pi_{\widehat{\boldsymbol{x}}}\,\boldsymbol{p}+\mathcal{O}\Big(\frac{|\boldsymbol{p}|}{|\boldsymbol{x}|}\Big)\Big)\,, \qquad \boldsymbol{p}\in\mathbb{C}^3\,,\ |\boldsymbol{x}|\to\infty\,,$$

(cf., e.g., [11, p. 208]) tell us that

$$\boldsymbol{U}_s(\boldsymbol{x}) \;=\; \frac{1}{4\pi}\frac{e^{\mathrm{i}|\boldsymbol{x}|}}{|\boldsymbol{x}|}\boldsymbol{A}_s(\widehat{\boldsymbol{x}})+\mathcal{O}(|\boldsymbol{x}|^{-2}) \qquad \text{as } |\boldsymbol{x}|\to\infty\,, \tag{18a}$$

$$\boldsymbol{U}_p(\boldsymbol{x}) \;=\; \frac{1}{4\pi}\frac{e^{\mathrm{i}|\boldsymbol{x}|}}{|\boldsymbol{x}|}\boldsymbol{A}_p(\widehat{\boldsymbol{x}})+\mathcal{O}(|\boldsymbol{x}|^{-2}) \qquad \text{as } |\boldsymbol{x}|\to\infty\,, \tag{18b}$$

where $\boldsymbol{A}_s \in L^2_t(S^2,\mathbb{C}^3)$ and $\boldsymbol{A}_p \in L^2_n(S^2,\mathbb{C}^3)$ are called *transversal* and *longitudinal elastic far fields* radiated by $\boldsymbol{F}$ and given by

$$\boldsymbol{A}_s(\boldsymbol{\theta}) \;=\; \Pi_{\boldsymbol{\theta}^\perp}\Big(\int_{\mathbb{R}^3} e^{-\mathrm{i}\boldsymbol{\theta}\cdot\boldsymbol{y}}\boldsymbol{F}(\boldsymbol{y})\,\mathrm{d}\boldsymbol{y}\Big)\,, \quad \boldsymbol{A}_p(\boldsymbol{\theta}) \;=\; \Pi_{\boldsymbol{\theta}}\Big(\int_{\mathbb{R}^3} e^{-\mathrm{i}\boldsymbol{\theta}\cdot\boldsymbol{y}}\boldsymbol{F}(\boldsymbol{y})\,\mathrm{d}\boldsymbol{y}\Big)\,, \qquad \boldsymbol{\theta}\in S^2\,,$$

i.e., the vector fields $\boldsymbol{A}_s$ and $\boldsymbol{A}_p$ are just the tangential and the normal components of the Fourier transform of the source $\boldsymbol{F}$ evaluated on the unit sphere S^2.

Accordingly, the *transversal* and *longitudinal elastic far field operators* $\mathcal{F}^{(s)}_{\text{elastic}}$ and $\mathcal{F}^{(p)}_{\text{elastic}}$, which map compactly supported body force densities to their radiated transversal and longitudinal elastic far fields, are the *tangential* and *normal projected restricted Fourier transforms*,

$$\mathcal{F}^{(s)}_{\text{elastic}} : L^2_0(\mathbb{R}^3,\mathbb{C}^3)\to L^2_t(S^2,\mathbb{C}^3)\,, \quad \mathcal{F}^{(s)}_{\text{elastic}}\boldsymbol{F} := \Pi_t(\widehat{\boldsymbol{F}}|_{S^2})\,, \tag{20a}$$

$$\mathcal{F}^{(p)}_{\text{elastic}} : L^2_0(\mathbb{R}^3,\mathbb{C}^3)\to L^2_n(S^2,\mathbb{C}^3)\,, \quad \mathcal{F}^{(p)}_{\text{elastic}}\boldsymbol{F} := \Pi_n(\widehat{\boldsymbol{F}}|_{S^2})\,. \tag{20b}$$

4. Projected restricted Fourier transforms

We continue by characterizing far fields radiated by electromagnetic or elastic sources supported in a ball $B_R(0)$ of radius $R>0$ centered at the origin. The similarity between (14) and (20) allows us to treat both cases in a unified framework, and we consider the *projected restricted Fourier transforms*

$$\mathcal{F}^{(t)}_{B_R(0)} : L^2(B_R(0),\mathbb{C}^3)\to L^2_t(S^2,\mathbb{C}^3)\,, \quad \mathcal{F}^{(t)}_{B_R(0)}\boldsymbol{f} := \Pi_t(\widehat{\boldsymbol{f}}|_{S^2})\,, \tag{21a}$$

$$\mathcal{F}^{(n)}_{B_R(0)} : L^2(B_R(0),\mathbb{C}^3)\to L^2_n(S^2,\mathbb{C}^3)\,, \quad \mathcal{F}^{(p)}_{B_R(0)}\boldsymbol{f} := \Pi_n(\widehat{\boldsymbol{f}}|_{S^2})\,. \tag{21b}$$

We restrict the discussion to L^2-sources supported on balls $B_R(0)$, because in this special case we can explicitly derive the singular value decompositions of both operators in terms of spaces of *vector spherical harmonics*.

To begin with, we collect some basic facts on vector spherical harmonics (see, e.g., [2] for more details). Let $\mathbb{Y}_n$ denote the space of (scalar) *spherical harmonics* of degree $n\geq 0$ on the unit sphere S^2. The subspaces $\mathbb{Y}_n$, $n\geq 0$, have dimension $2n+1$, are mutually orthogonal and span $L^2(S^2,\mathbb{C})$, i.e.,

$$L^2(S^2,\mathbb{C}) \;=\; \bigoplus_{n=0}^{\infty}\mathbb{Y}_n\,. \tag{22}$$

If we define, for $n \geq 1$,

$$\mathbb{U}_n := \mathbf{Grad}\, \mathbb{Y}_n \qquad \text{and} \qquad \mathbb{V}_n := -\mathbf{Curl}\, \mathbb{Y}_n = \boldsymbol{\nu} \times \mathbb{U}_n\,,$$

then $\mathbb{U}_n$ and $\mathbb{V}_n$ are mutually orthogonal, $\mathbb{T}_n := \mathbb{U}_n \oplus \mathbb{V}_n$ is called the space of *tangential vector spherical harmonics* of order n, and

$$L^2_t(S^2, \mathbb{C}^3) \;=\; \bigoplus_{n=1}^{\infty} \mathbb{T}_n\,.$$

Similarly, the space of *normal vector spherical harmonics* of order $n \geq 0$ is given by $\mathbb{W}_n := \boldsymbol{\nu}\mathbb{Y}_n$, and

$$L^2_n(S^2, \mathbb{C}^3) \;=\; \bigoplus_{n=0}^{\infty} \mathbb{W}_n\,.$$

If $\{Y_n^m \mid -n \leq m \leq n\}$ is any orthonormal basis of $\mathbb{Y}_n$, then

$$\boldsymbol{U}_n^m \;:=\; \frac{1}{\sqrt{n(n+1)}} \mathbf{Grad}\, Y_n^m\,, \qquad -n \leq m \leq n\,, \tag{23a}$$

$$\boldsymbol{V}_n^m \;:=\; -\frac{1}{\sqrt{n(n+1)}} \mathbf{Curl}\, Y_n^m = \boldsymbol{\nu} \times \boldsymbol{U}_n^m\,, \qquad -n \leq m \leq n\,, \tag{23b}$$

form orthonormal bases of $\mathbb{U}_n$ and $\mathbb{V}_n$, respectively, and $\{\boldsymbol{\nu} Y_n^m \mid -n \leq m \leq n\}$ is an orthonormal basis of $\mathbb{W}_n$.

4.1. The singular value decomposition of $\mathcal{F}^{(t)}_{B_R(0)}$

To formulate the singular value decomposition of the tangential restricted Fourier transform $\mathcal{F}^{(t)}_{B_R(0)}$ we use the *spherical vector wave functions*

$$\begin{aligned}
\boldsymbol{M}_n^m(\boldsymbol{x}) \;&:=\; -\sqrt{n(n+1)}\, j_n(|\boldsymbol{x}|) \boldsymbol{V}_n^m(\widehat{\boldsymbol{x}})\,, && \boldsymbol{x} \in \mathbb{R}^3\,,\\
\boldsymbol{N}_n^m(\boldsymbol{x}) \;&:=\; -\sqrt{n(n+1)}\, h_n^{(1)}(|\boldsymbol{x}|) \boldsymbol{V}_n^m(\widehat{\boldsymbol{x}})\,, && \boldsymbol{x} \in \mathbb{R}^3 \setminus \{0\}\,,
\end{aligned}$$

where j_n and $h_n^{(1)}$ denote the spherical Bessel and Hankel functions of degree n. These satisfy

$$\begin{aligned}
\mathbf{curl}\boldsymbol{M}_n^m(\boldsymbol{x}) \;&=\; \frac{n(n+1)}{|\boldsymbol{x}|} j_n(|\boldsymbol{x}|) Y_n^m(\widehat{\boldsymbol{x}}) \widehat{\boldsymbol{x}}\\
&\quad + \frac{\sqrt{n(n+1)}}{|\boldsymbol{x}|} (j_n(|\boldsymbol{x}|) + |\boldsymbol{x}| j_n'(|\boldsymbol{x}|)) \boldsymbol{U}_n^m(\widehat{\boldsymbol{x}})\,, && \boldsymbol{x} \in \mathbb{R}^3\,,\\
\mathbf{curl}\boldsymbol{N}_n^m(\boldsymbol{x}) \;&=\; \frac{n(n+1)}{|\boldsymbol{x}|} h_n^{(1)}(|\boldsymbol{x}|) Y_n^m(\widehat{\boldsymbol{x}}) \widehat{\boldsymbol{x}}\\
&\quad + \frac{\sqrt{n(n+1)}}{|\boldsymbol{x}|} (h_n^{(1)}(|\boldsymbol{x}|) + |\boldsymbol{x}| (h_n^{(1)})'(|\boldsymbol{x}|)) \boldsymbol{U}_n^m(\widehat{\boldsymbol{x}})\,, && \boldsymbol{x} \in \mathbb{R}^3 \setminus \{0\}\,,
\end{aligned}$$

(see, e.g., [14, Thm. 2.43]). Since $\boldsymbol{N}_n^m$ and $\mathbf{curl}\boldsymbol{N}_n^m$ are radiating solutions to the homogeneous Maxwell system in $\mathbb{R}^3 \setminus \{0\}$, they have a well-defined far field, and the

asymptotics of the spherical Hankel functions tell us that[2]

$$(\boldsymbol{N}_n^m)^\infty(\boldsymbol{\theta}) \;=\; -\frac{4\pi}{\mathrm{i}^{n+1}}\sqrt{n(n+1)}\boldsymbol{V}_n^m(\boldsymbol{\theta})\,, \qquad \boldsymbol{\theta}\in S^2\,, \tag{26a}$$

$$(\mathbf{curl}\boldsymbol{N}_n^m)^\infty(\boldsymbol{\theta}) \;=\; \frac{4\pi}{\mathrm{i}^{n}}\sqrt{n(n+1)}\boldsymbol{U}_n^m(\boldsymbol{\theta})\,, \qquad \boldsymbol{\theta}\in S^2\,, \tag{26b}$$

(cf., e.g., [2, Thm. 6.28]). Furthermore, for $n, n'\geq 1$, $-n\leq m\leq n$ and $-n'\leq m'\leq n'$, a short computation shows the orthogonality relations[3]

$$\int_{B_R(0)} \boldsymbol{M}_n^m(\boldsymbol{y})\cdot\overline{\boldsymbol{M}_{n'}^{m'}(\boldsymbol{y})}\,\mathrm{d}\boldsymbol{y} \;=\; \delta_m^{m'}\delta_n^{n'}n(n+1)\int_0^R j_n^2(r)r^2\,\mathrm{d}r\,,$$

$$\int_{B_R(0)} \mathbf{curl}\boldsymbol{M}_n^m(\boldsymbol{y})\cdot\overline{\mathbf{curl}\boldsymbol{M}_{n'}^{m'}(\boldsymbol{y})}\,\mathrm{d}\boldsymbol{y}$$

$$= \;\delta_m^{m'}\delta_n^{n'}n(n+1)\int_{B_R(0)}(n(n+1)j_n^2(r)+(j_n(r)+rj_n'(r))^2)\,\mathrm{d}r\,,$$

$$\int_{B_R(0)} \boldsymbol{M}_n^m(\boldsymbol{y})\cdot\overline{\mathbf{curl}\boldsymbol{M}_{n'}^{m'}(\boldsymbol{y})}\,\mathrm{d}\boldsymbol{y} \;=\; 0\,.$$

It is well known that, for any $\boldsymbol{p}\in\mathbb{C}^3$,

$$\begin{aligned}\mathbf{curl}_x\,\mathbf{curl}_x(\Phi(\boldsymbol{x}-\boldsymbol{y})\boldsymbol{p}) \;=\; &\mathrm{i}\sum_{n=1}^\infty\frac{1}{n(n+1)}\sum_{m=-n}^n \boldsymbol{N}_n^m(\boldsymbol{x})\overline{\boldsymbol{M}_n^m(\boldsymbol{y})}\cdot\boldsymbol{p}\\ &+\mathrm{i}\sum_{n=1}^\infty\frac{1}{n(n+1)}\sum_{m=-n}^n \mathbf{curl}\boldsymbol{N}_n^m(\boldsymbol{x})\overline{\mathbf{curl}\boldsymbol{M}_n^m(\boldsymbol{y})}\cdot\boldsymbol{p}\end{aligned}$$

(cf., e.g., [2, p. 222]), and using (26) we find that its far field satisfies

$$\begin{aligned}(\mathbf{curl}_x\,\mathbf{curl}_x(\Phi(\cdot-\boldsymbol{y})\boldsymbol{p}))^\infty(\boldsymbol{\theta}) \;=\; &-\sum_{n=1}^\infty\frac{4\pi}{i^n}\frac{1}{\sqrt{n(n+1)}}\sum_{m=-n}^n \boldsymbol{V}_n^m(\boldsymbol{\theta})\overline{\boldsymbol{M}_n^m(\boldsymbol{y})}\cdot\boldsymbol{p}\\ &+\sum_{n=1}^\infty\frac{4\pi}{i^{n-1}}\frac{1}{\sqrt{n(n+1)}}\sum_{m=-n}^n \boldsymbol{U}_n^m(\boldsymbol{\theta})\overline{\mathbf{curl}\boldsymbol{M}_n^m(\boldsymbol{y})}\cdot\boldsymbol{p}\,.\end{aligned}$$

Substituting this into (21) using (11)–(13) we obtain that

$$\begin{aligned}(\mathcal{F}_{B_R(0)}^{(t)}\boldsymbol{f})(\boldsymbol{\theta}) \;&=\; \int_{B_R(0)}(\mathbf{curl}_x\,\mathbf{curl}_x(\Phi(\cdot-\boldsymbol{y})\boldsymbol{f}(\boldsymbol{y})))^\infty(\boldsymbol{\theta})\,\mathrm{d}\boldsymbol{y}\\ &=\; -\sum_{n=1}^\infty\frac{4\pi}{\mathrm{i}^n}\frac{1}{\sqrt{n(n+1)}}\sum_{m=-n}^n \boldsymbol{V}_n^m(\boldsymbol{\theta})\int_{B_R(0)}\overline{\boldsymbol{M}_n^m(\boldsymbol{y})}\cdot\boldsymbol{f}(\boldsymbol{y})\,\mathrm{d}\boldsymbol{y}\\ &\quad+\sum_{n=1}^\infty\frac{4\pi}{\mathrm{i}^{n-1}}\frac{1}{\sqrt{n(n+1)}}\sum_{m=-n}^n \boldsymbol{U}_n^m(\boldsymbol{\theta})\int_{B_R(0)}\overline{\mathbf{curl}\boldsymbol{M}_n^m(\boldsymbol{y})}\cdot\boldsymbol{f}(\boldsymbol{y})\,\mathrm{d}\boldsymbol{y}\,.\end{aligned}$$

Since $\boldsymbol{U}_n^m, \boldsymbol{V}_n^m$, $n\geq 1$, $-n\leq m\leq n$, form a complete orthonormal system in $L_t^2(S^2,\mathbb{C}^3)$, and $\boldsymbol{M}_n^m, \mathbf{curl}\boldsymbol{M}_n^m$, $n\geq 1$, $-n\leq m\leq n$, is an orthogonal system in $L^2(B_R(0),\mathbb{C}^3)$,

[2] Sometimes we denote the far field of a radiating solution $\boldsymbol{U}$ to Maxwell's equations or of the Navier system just by $\boldsymbol{U}^\infty$.

[3] As usual, $\delta_n^{n'}$, $n,n'\in\mathbb{Z}$ denotes the Kronecker delta.

this shows that a singular system for $\mathcal{F}^{(t)}_{B_R(0)}$ is given by $(\sigma^{(j)}_{m,n}; \boldsymbol{u}^{(j)}_{m,n}, \boldsymbol{v}^{(j)}_{m,n})$, $n \geq 1$, $-n \leq m \leq n$, $j = s, t$, where the squared singular values $(\sigma^{(j)}_{m,n})^2$ are[4]

$$(\sigma^{(s)}_{m,n})^2 \;:=\; 4\pi r_n^2(R) \;:=\; (4\pi)^2 \int_0^R \big(n(n+1) j_n^2(r) + (j_n(r) + r j_n'(r))^2\big)\, \mathrm{d}r\,, \tag{28a}$$

$$(\sigma^{(t)}_{m,n})^2 \;:=\; 4\pi s_n^2(R) \;:=\; (4\pi)^2 \int_0^R j_n^2(r) r^2\, \mathrm{d}r\,, \tag{28b}$$

the left singular vectors are

$$\boldsymbol{u}^{(s)}_{m,n}(\boldsymbol{\theta}) \;:=\; \boldsymbol{U}^m_n(\boldsymbol{\theta})\,, \quad \boldsymbol{u}^{(t)}_{m,n}(\boldsymbol{\theta}) \;:=\; \boldsymbol{V}^m_n(\boldsymbol{\theta})\,, \qquad \boldsymbol{\theta} \in S^2\,, \tag{28c}$$

and the right singular vectors are

$$\boldsymbol{v}^{(s)}_{m,n}(\boldsymbol{y}) \;:=\; \Big(\frac{4\pi}{n(n+1)}\Big)^{\frac{1}{2}} \frac{\mathrm{i}^{n-1}}{r_n(R)} \mathbf{curl} \boldsymbol{M}^m_n(\boldsymbol{y})\,, \qquad \boldsymbol{y} \in B_R(0)\,, \tag{28d}$$

$$\boldsymbol{v}^{(t)}_{m,n}(\boldsymbol{y}) \;:=\; -\Big(\frac{4\pi}{n(n+1)}\Big)^{\frac{1}{2}} \frac{\mathrm{i}^{n}}{s_n(R)} \boldsymbol{M}^m_n(\boldsymbol{y})\,, \qquad \boldsymbol{y} \in B_R(0)\,. \tag{28e}$$

Remark 4.1. The *rescaled squared singular values* $\{s_n^2(R)\}$ of the operator $\mathcal{F}^{(t)}_{B_R(0)}$ in (28b) coincide with the rescaled squared singular values of the corresponding operator in our study of the three-dimensional scalar case in [8]. These numbers have been analyzed in [8], and a corresponding analysis of the rescaled squared singular values $\{r_n^2(R)\}$ from (28a) can be found in Appendix A below. The following properties will have immediate consequences for our subsequent analysis.

The numbers $\{r_n^2(R)\}$ and $\{s_n^2(R)\}$ satisfy

$$\sum_{n=0}^{\infty} (2n+1) r_n^2(R) \;=\; \frac{4\pi}{3} R^3 + 4\pi R \qquad \text{and} \qquad \sum_{n=0}^{\infty} (2n+1) s_n^2(R) \;=\; \frac{4\pi}{3} R^3\,,$$

but they decay rapidly as a function of n as soon as $n \gtrsim R$,

$$r_n^2(R) \;\leq\; b_0 \Big(3\sqrt{e} \max\Big\{1, \frac{1}{R}\Big\} + R + \frac{2\sqrt{e}}{R}\Big) \Big(n + \frac{3}{2}\Big)^{\frac{2}{3}} \Big(\frac{R^2}{n^2} e^{1 - \frac{R^2}{(n+2)^2}}\Big)^n \qquad \text{if } n \geq R > 0\,,$$

$$s_n^2(R) \;\leq\; b_0 R \Big(n + \frac{1}{2}\Big)^{\frac{2}{3}} \Big(\frac{R^2}{(n+1)^2} e^{1 - \frac{R^2}{(n+1)^2}}\Big)^{n+1} \qquad \text{if } n \geq R > 0\,,$$

where the constant $b_0 \approx 4.791$ is independent of n and R. Moreover, the odd and even rescaled squared singular values $r_{2n+1}^2(R)$, $s_{2n+1}^2(R)$ and $r_{2n}^2(R)$, $s_{2n}^2(R)$ are decreasing as functions of n, and for $n \geq R$ both sequences $r_n^2(R)$ and $s_n^2(R)$ are strictly monotonically decreasing as a whole. Asymptotically, as $R \to \infty$,

$$r_n^2(R) \;\sim\; s_n^2(R) \;\sim\; \begin{cases} 2\pi \sqrt{R^2 - \Big(n + \frac{1}{2}\Big)^2}\,, & n + \frac{1}{2} \leq R\ , \\ 0\,, & n + \frac{1}{2} > R\ , \end{cases}$$

(see also Lemma A.6 below and [8, Cor. A.10] for more rigorous statements).

[4] The superscripts (s) and (t) refer to the fact that the corresponding left singular vectors $\boldsymbol{u}^{(s)}_{m,n}$ and $\boldsymbol{u}^{(t)}_{m,n}$ in (28c) are sometimes said to be spheroidal and toroidal tangential vector fields, respectively, (see, e.g., [4, p. 223]).

This means that there is an approximately $2R^2$-dimensional subspace of $L^2(B_R(0),\mathbb{C}^3)$ that is propagated by $\mathcal{F}^{(t)}_{B_R(0)}$, while its orthogonal complement is strongly dampened. We will utilize this rapid transition to evanescence to define subspaces of so-called nonevanescent far fields as part of our regularization strategy for far field splitting and data completion in Section 4.4 below. ◊

4.2. The singular value decomposition of $\mathcal{F}^{(n)}_{B_R(0)}$

To formulate the singular value decomposition of the normal restricted Fourier transform $\mathcal{F}^{(n)}_{B_R(0)}$ we use the *spherical wave functions*

$$u_n^m(\boldsymbol{x}) := j_n(|\boldsymbol{x}|)Y_n^m(\widehat{\boldsymbol{x}})\,, \quad \boldsymbol{x}\in\mathbb{R}^3\,, \qquad v_n^m(\boldsymbol{x}) := h_n^{(1)}(|\boldsymbol{x}|)Y_n^m(\widehat{\boldsymbol{x}})\,, \quad \boldsymbol{x}\in\mathbb{R}^3\setminus\{0\}\,.$$

For any $\boldsymbol{p}\in\mathbb{C}^3$,

$$\nabla_{\boldsymbol{x}}\operatorname{div}_{\boldsymbol{x}}(\Phi(\boldsymbol{x}-\boldsymbol{y})\boldsymbol{p}) = \mathrm{i}\sum_{n=0}^{\infty}\sum_{m=-n}^{n}\nabla v_n^m(\boldsymbol{x})\overline{\nabla u_n^m(\boldsymbol{y})}\cdot\boldsymbol{p}$$

(cf., e.g., [2, p. 222]). The asymptotics of the spherical Hankel functions (cf., e.g., [2, p. 31]) tell us that

$$\nabla v_n^m(\boldsymbol{x}) = \frac{1}{4\pi}\frac{e^{\mathrm{i}|\boldsymbol{x}|}}{|\boldsymbol{x}|}\frac{4\pi}{\mathrm{i}^n}Y_n^m(\widehat{\boldsymbol{x}})\widehat{\boldsymbol{x}}+\mathcal{O}(|\boldsymbol{x}|^{-2}) \qquad \text{as } |\boldsymbol{x}|\to\infty\,,$$

i.e.,

$$(\nabla_{\boldsymbol{x}}\operatorname{div}_{\boldsymbol{x}}(\Phi(\cdot-\boldsymbol{y})\boldsymbol{p})^\infty(\boldsymbol{\theta}) = \sum_{n=0}^{\infty}\sum_{m=-n}^{n}\frac{4\pi}{\mathrm{i}^{n-1}}Y_n^m(\boldsymbol{\theta})\boldsymbol{\theta}\,\overline{\nabla u_n^m(\boldsymbol{y})}\cdot\boldsymbol{p}\,.$$

Substituting this into (21) and using (17)–(18) we obtain that

$$\begin{aligned}(\mathcal{F}^{(n)}_{B_R(0)}\boldsymbol{f})(\boldsymbol{\theta}) &= \int_{B_R(0)}(\nabla_{\boldsymbol{x}}\operatorname{div}_{\boldsymbol{x}}(\Phi(\cdot-\boldsymbol{y})\boldsymbol{f}(\boldsymbol{y}))^\infty(\boldsymbol{\theta})\,\mathrm{d}\boldsymbol{y}\\ &= \sum_{n=0}^{\infty}\frac{4\pi}{\mathrm{i}^{n-1}}\sum_{m=-n}^{n}Y_n^m(\boldsymbol{\theta})\boldsymbol{\theta}\int_{B_R(0)}\overline{\nabla u_n^m(\boldsymbol{y})}\cdot\boldsymbol{f}(\boldsymbol{y})\,\mathrm{d}\boldsymbol{y}\,.\end{aligned}$$

For $n,n'\geq 0$, $-n\leq m\leq n$ and $-n'\leq m'\leq n'$, a short computation shows the orthogonality relation

$$\int_{B_R(0)}\nabla u_n^m(\boldsymbol{y})\cdot\overline{\nabla u_{n'}^{m'}(\boldsymbol{y})}\,\mathrm{d}\boldsymbol{y} = \delta_m^{m'}\delta_n^{n'}\int_0^R(n(n+1)j_n^2(r)+(rj_n'(r))^2)\,\mathrm{d}r\,.$$

Therefore, a singular system for $\mathcal{F}^{(n)}_{B_R(0)}$ is given by $(\sigma^{(n)}_{m,n};\boldsymbol{u}^{(n)}_{m,n},\boldsymbol{v}^{(n)}_{m,n})$, $-n\leq m\leq n$, $n\geq 0$, where the squared singular values $(\sigma^{(n)}_{m,n})^2$ are

$$(\sigma^{(n)}_{m,n})^2 := 4\pi t_n^2(R) := (4\pi)^2\int_0^R(n(n+1)j_n^2(r)+(rj_n'(r))^2)\,\mathrm{d}r\,, \tag{30a}$$

the left singular vectors are

$$\boldsymbol{u}^{(n)}_{m,n}(\boldsymbol{\theta}) := Y_n^m(\boldsymbol{\theta})\boldsymbol{\theta}\,, \qquad \boldsymbol{\theta}\in S^2\,, \tag{30b}$$

and the right singular vectors are

$$\boldsymbol{v}^{(n)}_{m,n}(\boldsymbol{y}) := \frac{\sqrt{4\pi}\,\mathrm{i}^{n-1}}{t_n(R)}\nabla u_n^m(\boldsymbol{y})\,, \qquad \boldsymbol{y}\in B_R(0)\,. \tag{30c}$$

Remark 4.2. The *rescaled squared singular values* $t_n^2(R)$ of the operator $\mathcal{F}^{(n)}_{B_R(0)}$ show the same qualitative behavior as the rescaled squared singular values of the tangential restricted Fourier transform considered in Section 4.1. Proofs of the following results can be found in Appendix A.

The numbers $\{t_n^2(R)\}$ satisfy

$$\sum_{n=0}^{\infty}(2n+1)t_n^2(R) \;=\; \frac{4\pi}{3}R^3\,,$$

but they decay rapidly as a function of n as soon as $n \gtrsim R$,

$$t_n^2(R) \;\le\; b_0\Big(3\sqrt{e}\max\Big\{1,\frac{1}{R}\Big\}+R\Big)\Big(n+\frac{3}{2}\Big)^{\frac{2}{3}}\Big(\frac{R^2}{n^2}e^{1-\frac{R^2}{(n+2)^2}}\Big)^n \qquad \text{if } n \ge R > 0\,,$$

where the constant $b_0 \approx 4.791$ is independent of n and R. Moreover, the odd and even rescaled squared singular values $t_{2n+1}^2(R)$ and $t_{2n}^2(R)$ are decreasing as functions of n, and for $n \ge R$ the sequence $t_n^2(R)$ is strictly monotonically decreasing as a whole. Asymptotically, as $R \to \infty$,

$$t_n^2(R) \;\sim\; \begin{cases} 2\pi\sqrt{R^2-\Big(n+\frac{1}{2}\Big)^2}\,, & n+\frac{1}{2} \le R\ , \\ 0\,, & n+\frac{1}{2} > R\ , \end{cases}$$

(see also Lemma A.6 for a more rigorous statement). ◊

4.3. Expansions into spherical harmonics and vector spherical harmonics

Next we consider expansions of vector fields on the sphere into left singular vectors of the restricted Fourier transforms $\mathcal{F}^{(t)}_{B_R(0)}$ and $\mathcal{F}^{(n)}_{B_R(0)}$, i.e., into tangential and normal vector spherical harmonics. This gives sparse representations of far fields of time-harmonic electromagnetic and elastic waves radiated by compactly supported sources that will be used in Sections 5–6 below to analyze far field splitting and data completion.

According to (22), any $\alpha \in L^2(S^2,\mathbb{C})$ can be uniquely represented as a sum of spherical harmonics,

$$\alpha \;=\; \sum_{n=0}^{\infty}\alpha_n\,, \qquad \alpha_n \in \mathbb{Y}_n\,, \tag{31}$$

and the *n-spherical harmonic component* $\alpha_n \in \mathbb{Y}_n$ of α is given by

$$\alpha_n(\boldsymbol{\theta}) \;=\; (\mathcal{P}_n\alpha)(\boldsymbol{\theta}) \;:=\; \frac{2n+1}{4\pi}\int_{S^2} P_n(\boldsymbol{\theta}\cdot\boldsymbol{\omega})\alpha(\boldsymbol{\omega})\,\mathrm{d}s(\boldsymbol{\omega})\,, \qquad \boldsymbol{\theta}\in S^2\,, \tag{32}$$

where $\mathcal{P}_n : L^2(S^2,\mathbb{C}) \to L^2(S^2,\mathbb{C})$ denotes the orthogonal projection onto $\mathbb{Y}_n$, and P_n is the Legendre polynomial of degree n (see, e.g., [1, p. 26]). As a consequence, we have the Parseval identity

$$\|\alpha\|^2_{L^2(S^2,\mathbb{C})} \;=\; \sum_{n=0}^{\infty}\|\alpha_n\|^2_{L^2(S^2,\mathbb{C})}\,, \qquad \alpha \in L^2(S^2,\mathbb{C})\,,$$

and the sequence of spherical harmonic components of α satisfies $\{\alpha_n\} \in \ell^2(L^2(S^2,\mathbb{C}))$, where

$$\ell^2(L^2(S^2,\mathbb{C})) := \{\{\beta_n\} \mid \beta_n \in \mathbb{Y}_n \text{ for all } n \in \mathbb{N} \text{ and } \sum_{n=0}^{\infty} \|\beta_n\|^2_{L^2(S^2,\mathbb{C})} < \infty\}\,.$$

It is sometimes useful to think of the projection kernel in (32) as a function of $\boldsymbol{\theta}$ for each fixed $\boldsymbol{\omega} \in S^2$, and we use the notation $P_n^{\boldsymbol{\omega}}(\boldsymbol{\theta}) := P_n(\boldsymbol{\theta}\cdot\boldsymbol{\omega})$ to emphasize this point of view. We note that $P_n^{\boldsymbol{\omega}}(\boldsymbol{\theta})$ is itself a spherical harmonic of degree n that satisfies

$$\|P_n^{\boldsymbol{\omega}}\|_{L^2(S^2,\mathbb{C})} = \sqrt{\frac{4\pi}{2n+1}} \qquad \text{and} \qquad \|P_n^{\boldsymbol{\omega}}\|_{L^\infty(S^2,\mathbb{C})} = 1\,, \tag{33}$$

independent of $\boldsymbol{\omega} \in S^2$ (cf. [1, (2.39)–(2.40)]).

Next, given any smooth tangential vector field $\boldsymbol{A} \in L^2_t(S^2,\mathbb{C}^3)$ the functions $\mathrm{Div}\boldsymbol{A}$, $\mathrm{Curl}\,\boldsymbol{A} \in L^2(S^2,\mathbb{C})$ can be uniquely represented as a sum of spherical harmonics, and using (31)–(32) and (3) we find that

$$\begin{aligned}
\mathrm{Div}\boldsymbol{A}(\boldsymbol{\theta}) &= -\sum_{n=1}^{\infty} \frac{2n+1}{4\pi} \int_{S^2} (\mathbf{Grad}^T_{\boldsymbol{\omega}} P_n(\boldsymbol{\theta}\cdot\boldsymbol{\omega}))\boldsymbol{A}(\boldsymbol{\omega})\, \mathrm{d}s(\boldsymbol{\omega})\,,\\
\mathrm{Curl}\,\boldsymbol{A}(\boldsymbol{\theta}) &= \sum_{n=1}^{\infty} \frac{2n+1}{4\pi} \int_{S^2} (\mathbf{Curl}^T_{\boldsymbol{\omega}} P_n(\boldsymbol{\theta}\cdot\boldsymbol{\omega}))\boldsymbol{A}(\boldsymbol{\omega})\, \mathrm{d}s(\boldsymbol{\omega})\,.
\end{aligned}$$

Accordingly (cf., e.g., the proof of Theorem 6.25 in [2]),

$$\begin{aligned}
\boldsymbol{A}(\boldsymbol{\theta}) = \sum_{n=1}^{\infty} \frac{2n+1}{4\pi} \frac{1}{n(n+1)} \Big(&\int_{S^2} (\mathbf{Grad}_{\boldsymbol{\theta}} \mathbf{Grad}^T_{\omega} P_n(\boldsymbol{\theta}\cdot\boldsymbol{\omega}))\boldsymbol{A}(\boldsymbol{\omega})\, \mathrm{d}s(\boldsymbol{\omega})\\
&+ \int_{S^2} (\mathbf{Curl}_{\boldsymbol{\theta}} \mathbf{Curl}^T_{\omega} P_n(\boldsymbol{\theta}\cdot\boldsymbol{\omega}))\boldsymbol{A}(\boldsymbol{\omega})\, \mathrm{d}s(\boldsymbol{\omega}) \Big)\,.
\end{aligned}$$

Using a density argument, this implies that any $\boldsymbol{A} \in L^2_t(S^2,\mathbb{C}^3)$ can be uniquely represented as a sum of tangential spherical vector harmonics

$$\boldsymbol{A} = \sum_{n=1}^{\infty} \boldsymbol{A}_n\,, \qquad \boldsymbol{A}_n \in \mathbb{T}_n\,, \tag{35}$$

and the *n-spherical vector harmonic component* $\boldsymbol{A}_n \in \mathbb{T}_n$ of $\boldsymbol{A}$ is given by $\boldsymbol{A}_n = \boldsymbol{A}_n^{(s)} + \boldsymbol{A}_n^{(t)} \in \mathbb{U}_n \oplus \mathbb{V}_n$ with

$$\boldsymbol{A}_n^{(s)}(\boldsymbol{\theta}) = (\boldsymbol{\mathcal{P}}_n^{(s)}\boldsymbol{A})(\boldsymbol{\theta}) := \frac{2n+1}{4\pi} \int_{S^2} \boldsymbol{P}_n^{(s)}(\boldsymbol{\theta},\boldsymbol{\omega})\boldsymbol{A}(\boldsymbol{\omega})\, \mathrm{d}s(\boldsymbol{\omega})\,, \qquad \boldsymbol{\theta} \in S^2\,, \tag{36a}$$

$$\boldsymbol{A}_n^{(t)}(\boldsymbol{\theta}) = (\boldsymbol{\mathcal{P}}_n^{(t)}\boldsymbol{A})(\boldsymbol{\theta}) := \frac{2n+1}{4\pi} \int_{S^2} \boldsymbol{P}_n^{(t)}(\boldsymbol{\theta},\boldsymbol{\omega})\boldsymbol{A}(\boldsymbol{\omega})\, \mathrm{d}s(\boldsymbol{\omega})\,, \qquad \boldsymbol{\theta} \in S^2\,, \tag{36b}$$

where $\boldsymbol{\mathcal{P}}_n^{(s)} : L^2_t(S^2,\mathbb{C}^3) \to L^2_t(S^2,\mathbb{C}^3)$ and $\boldsymbol{\mathcal{P}}_n^{(t)} : L^2_t(S^2,\mathbb{C}^3) \to L^2_t(S^2,\mathbb{C}^3)$ denote the orthogonal projections onto $\mathbb{U}_n$ and $\mathbb{V}_n$, with projection kernels

$$\boldsymbol{P}_n^{(s)}(\boldsymbol{\theta},\boldsymbol{\omega}) := \frac{1}{n(n+1)} \mathbf{Grad}_{\boldsymbol{\theta}}\, \mathbf{Grad}^T_{\omega}\, P_n(\boldsymbol{\theta}\cdot\boldsymbol{\omega})\,, \qquad \boldsymbol{\theta},\boldsymbol{\omega} \in S^2\,, \tag{37a}$$

$$\boldsymbol{P}_n^{(t)}(\boldsymbol{\theta},\boldsymbol{\omega}) := \frac{1}{n(n+1)} \mathbf{Curl}_{\boldsymbol{\theta}}\, \mathbf{Curl}^T_{\omega}\, P_n(\boldsymbol{\theta}\cdot\boldsymbol{\omega})\,, \qquad \boldsymbol{\theta},\boldsymbol{\omega} \in S^2\,. \tag{37b}$$

We have the Parseval identity

$$\|\boldsymbol{A}\|^2_{L^2(S^2,\mathbb{C}^3)} \,=\, \sum_{n=1}^{\infty} \|\boldsymbol{A}_n\|^2_{L^2(S^2,\mathbb{C}^3)}\,, \qquad \boldsymbol{A}\in L^2_t(S^2,\mathbb{C}^3)\,, \tag{38}$$

and the sequence of vector spherical harmonic components of $\boldsymbol{A}$ satisfies $\{\boldsymbol{A}_n\}\in \ell^2(L^2_t(S^2,\mathbb{C}^3))$, where

$$\ell^2(L^2_t(S^2,\mathbb{C}^3)) \,:=\, \{\{\boldsymbol{B}_n\} \mid \boldsymbol{B}_n\in \mathbb{T}_n \text{ for all } n\geq 1 \text{ and } \sum_{n=1}^{\infty} \|\boldsymbol{B}_n\|^2_{L^2(S^2,\mathbb{C}^3)} <\infty\}\,.$$

As in the scalar case, we use the notation $\boldsymbol{P}_n^{(s,\boldsymbol{\omega})}(\boldsymbol{\theta}) := \boldsymbol{P}_n^{(s)}(\boldsymbol{\theta},\boldsymbol{\omega})$ and $\boldsymbol{P}_n^{(t,\boldsymbol{\omega})}(\boldsymbol{\theta}) := \boldsymbol{P}_n^{(t)}(\boldsymbol{\theta},\boldsymbol{\omega})$, when considering the projection kernels in (37) as functions of $\boldsymbol{\theta}$ for each fixed $\boldsymbol{\omega}\in S^2$. We note that each column of $\boldsymbol{P}_n^{(s,\boldsymbol{\omega})}$ and $\boldsymbol{P}_n^{(t,\boldsymbol{\omega})}$ are themselves tangential spherical vector harmonics of degree n that belong to $\mathbb{U}_n$ and $\mathbb{V}_n$, respectively. Furthermore, for $j=s,t$,

$$\|\boldsymbol{P}_n^{(j,\boldsymbol{\omega})}\|_{L^2(S^2,\mathbb{C}^{3\times 3})} \,=\, \sqrt{\frac{4\pi}{2n+1}} \qquad \text{and} \qquad \|\boldsymbol{P}_n^{(j,\boldsymbol{\omega})}\|_{L^\infty(S^2,\mathbb{C}^{3\times 3})} \,\leq\, \sqrt{3}\,, \tag{39}$$

independent of $\boldsymbol{\omega}\in S^2$ (see, e.g., [4, Sec. 5.9]). Here

$$\|\boldsymbol{F}\|_{L^2(S^2,\mathbb{C}^{3\times 3})} \,:=\, \Big(\int_{S^2} \|\boldsymbol{F}(\boldsymbol{\theta})\|_F^2 \,\mathrm{d}s(\boldsymbol{\theta})\Big)^{\frac{1}{2}}\,, \qquad \|\boldsymbol{F}\|_{L^\infty(S^2,\mathbb{C}^{3\times 3})} \,:=\, \operatorname*{ess\,sup}_{\boldsymbol{\theta}\in S^2} \|\boldsymbol{F}(\boldsymbol{\theta})\|_F\,,$$

and $\|\cdot\|_F$ denotes the Frobenius norm on $\mathbb{C}^{3\times 3}$.

Finally, since any normal vector field $\boldsymbol{A}\in L^2_n(S^2,\mathbb{C}^3)$ on the unit sphere can be rewritten as $\boldsymbol{A}=\boldsymbol{\nu}\alpha$ with $\alpha=\boldsymbol{\nu}\cdot\boldsymbol{A}\in L^2(S^2,\mathbb{C})$, the scalar spherical harmonic components $\{\alpha_n\}$ of α can be used to represent $\boldsymbol{A}$ as a sum of normal spherical vector harmonics

$$\boldsymbol{A} \,=\, \boldsymbol{\nu}\sum_{n=0}^{\infty} \alpha_n \qquad \text{with} \qquad \|\boldsymbol{A}\|^2_{L^2(S^2,\mathbb{C}^3)} \,=\, \sum_{n=0}^{\infty} \|\alpha_n\|^2_{L^2(S^2,\mathbb{C})}\,.$$

4.4. Regularized Picard criteria for $\mathcal{F}^{(t)}_{B_R(0)}$ and $\mathcal{F}^{(n)}_{B_R(0)}$

Using the singular value decompositions of the tangential and normal restricted Fourier transforms $\mathcal{F}^{(t)}_{B_R(0)}$ and $\mathcal{F}^{(n)}_{B_R(0)}$ established in (28) and (30), we now characterize far fields that can be radiated by limited power sources supported in the ball $B_R(0)$ of radius $R>0$ around the origin and at the same time can be detected by receivers with limited sensitivity.

We begin with the tangential restricted Fourier transform $\mathcal{F}^{(t)}_{B_R(0)}$. The singular value decomposition (28) shows that the source $\boldsymbol{f}^*_{\boldsymbol{A}}\in L^2(B_R(0),\mathbb{C}^3)$ with smallest L^2-norm that is supported in $B_R(0)$ and radiates a given tangential far field $\boldsymbol{A}\in L^2_t(S^2,\mathbb{C}^3)$, i.e., $\mathcal{F}^{(t)}_{B_R(0)}\boldsymbol{f}^*_{\boldsymbol{A}}=\boldsymbol{A}$, has L^2-norm

$$\|\boldsymbol{f}^*_{\boldsymbol{A}}\|^2_{L^2(B_R(0),\mathbb{C}^3)} \,=\, \frac{1}{4\pi}\sum_{n=1}^{\infty}\Big(\frac{\|\boldsymbol{A}_n^{(s)}\|^2_{L^2(S^2,\mathbb{C}^3)}}{r_n^2(R)} + \frac{\|\boldsymbol{A}_n^{(t)}\|^2_{L^2(S^2,\mathbb{C}^3)}}{s_n^2(R)}\Big)\,,$$

where $\{\boldsymbol{A}_n^{(s)}\}$ and $\{\boldsymbol{A}_n^{(t)}\}$ are the sequences of spheroidal and toroidal tangential vector spherical harmonic components of $\boldsymbol{A}$ from (36). In the following we refer to $\boldsymbol{f}_{\boldsymbol{A}}^*$ as the *minimal power source* radiating $\boldsymbol{A}$, and to $\|\boldsymbol{A}\|^2_{L^2(S^2,\mathbb{C}^3)}$ as the *radiated power* of the far field $\boldsymbol{A}$. Assuming that any relevant physical source has *limited power*, which we denote by $P > 0$, and that any available receiver has a *power threshold*, which we denote by $p > 0$ (i.e., the receiver cannot detect a far field that has power less than p), we define

$$N_s(R,P,p) := \inf\Big\{ n \in \mathbb{N} \;\Big|\; \Big(n+\frac{3}{2}\Big)^2 \geq R^2 + \frac{1}{4} \text{ and } 4\pi r_{n+1}^2(R) < \frac{p}{P} \Big\}, \tag{40a}$$

$$N_t(R,P,p) := \inf\Big\{ n \in \mathbb{N} \;\Big|\; \Big(n+\frac{3}{2}\Big)^2 \geq R^2 + \frac{1}{4} \text{ and } 4\pi s_{n+1}^2(R) < \frac{p}{P} \Big\}. \tag{40b}$$

Remark 4.3. The upper bounds for the rescaled squared singular values given in Lemma A.4 and Remark A.5 guarantee that $N_s(R,P,p)$ and $N_t(R,P,p)$ are always finite. The monotonicity results for the rescaled squared singular values established in Lemma A.2 and A.3 imply that

$$4\pi r_n^2(R) < \frac{p}{P} \quad \text{for all } n > N_s(R,P,p)\,, \qquad 4\pi s_n^2(R) < \frac{p}{P} \quad \text{for all } n > N_t(R,P,p)\,,$$

and

$$4\pi r_n^2(R) \geq \frac{p}{P} \quad \text{for all } n \leq N_s(R,P,p)\,, \qquad 4\pi s_n^2(R) \geq \frac{p}{P} \quad \text{for all } n \leq N_t(R,P,p)\,.$$

Furthermore, for $\nu := n + \frac{1}{2} \leq R$, we obtain from (A.1), (A.2), and (A.4) that

$$r_n^2(R) \;\geq\; s_n^2(R) \;=\; 2\pi \int_0^R J_\nu^2(r) r \,\mathrm{d}r \;\geq\; 2\pi \int_0^\nu J_\nu^2(r) r \,\mathrm{d}r\,.$$

Applying [21, 10.22.27], and the fact that $\nu J_\nu^2(\nu)$ as well as $\frac{J_{\nu+1}^2(\nu)}{J_\nu^2(\nu)}$ are monotonically increasing as functions of ν (see [27, p. 260] and [20, Thm. 3]), we obtain that, for $\frac{3}{2} \leq \nu \leq R$,

$$\begin{aligned} 4\pi r_n^2(R) \;\geq\; 4\pi s_n^2(R) \;&\geq\; 8\pi(\nu+1) J_{\nu+1}^2(\nu) \;\geq\; 8\pi\nu J_\nu^2(\nu) \frac{J_{\nu+1}^2(\nu)}{J_\nu^2(\nu)} \\ &\geq\; 8\pi J_{\frac{5}{2}}^2\Big(\frac{3}{2}\Big) \;\approx\; 0.389\,. \end{aligned}$$

This suggests that for reasonable values of $\frac{p}{P} \ll 1$ the assumption $(n+\frac{3}{2}) \geq R^2 + \frac{1}{4}$ in (40) is always satisfied.

Since the rescaled squared singular values $r_n^2(R)$ and $s_n^2(R)$ decrease very rapidly for $|n| \gtrsim R$, the numbers $N_s(R,P,p)$ and $N_t(R,P,p)$ are only a little larger than R for a wide range of P and p. ◊

Accordingly, if $\boldsymbol{A} \in L_t^2(S^2,\mathbb{C}^3)$ is a tangential far field with spheroidal and toroidal vector spherical harmonic components $\{\boldsymbol{A}_n^{(s)}\}$ and $\{\boldsymbol{A}_n^{(t)}\}$ radiated by a limited power source supported in $B_R(0)$ with $\|\boldsymbol{f}_{\boldsymbol{A}}^*\|^2_{L^2(B_R(0),\mathbb{C}^3)} \leq P$, then, for $N_s = N_s(R,P,p)$ and $N_t = N_t(R,P,p)$,

$$P \;\geq\; \frac{1}{4\pi} \sum_{n>N_s} \frac{\|\boldsymbol{A}_n^{(s)}\|^2_{L^2(S^2,\mathbb{C}^3)}}{r_n^2(R)} \;>\; \frac{P}{p} \sum_{n>N_s} \|\boldsymbol{A}_n^{(s)}\|^2_{L^2(S^2,\mathbb{C}^3)}\,,$$

$$P \;\geq\; \frac{1}{4\pi} \sum_{n>N_t} \frac{\|\boldsymbol{A}_n^{(t)}\|^2_{L^2(S^2,\mathbb{C}^3)}}{s_n^2(R)} \;>\; \frac{P}{p} \sum_{n>N_t} \|\boldsymbol{A}_n^{(t)}\|^2_{L^2(S^2,\mathbb{C}^3)}\,.$$

Consequently, $\sum_{n>N_j} \|\boldsymbol{A}_n^{(j)}\|^2_{L^2(S^2,\mathbb{C}^3)} < p$, $j = s, t$, is below the power threshold, and the subspace of detectable tangential far fields, that can be radiated by a power limited source supported in $B_R(0)$ is given by

$$\mathbb{U}_{\leq N_s} \oplus \mathbb{V}_{\leq N_t} := \bigoplus_{n=1}^{N_s} \mathbb{U}_n \oplus \bigoplus_{n=1}^{N_t} \mathbb{V}_n \,.$$

We refer to $\mathbb{U}_{\leq N_s} \oplus \mathbb{V}_{\leq N_t} \subseteq L^2_t(S^2, \mathbb{C}^3)$ as the subspace of *nonevanescent tangential far fields*, and to the orthogonal projection of a tangential far field onto this subspace as the *nonevanescent part* of the far field.

Similarly, using the singular value decomposition (30) of the normal restricted Fourier transform $\mathcal{F}^{(n)}_{B_R(0)}$ and proceeding as before, we define

$$N_n(R, P, p) := \inf\Big\{ n \in \mathbb{N} \;\Big|\; \Big(n + \frac{3}{2}\Big)^2 \geq R^2 + \frac{1}{4} \;\text{ and }\; 4\pi t^2_{n+1}(R) < \frac{p}{P} \Big\},$$

denote by

$$\mathbb{W}_{\leq N_n} := \bigoplus_{n=0}^{N_n} \mathbb{W}_n$$

the subspace of *nonevanescent normal far fields*, and refer to the orthogonal projection of a normal far field onto this subspace as the *nonevanescent part* of the far field.

From now on our basic reasoning relies on the assumption that all relevant information about a far field radiated from $B_R(0)$ is contained in its nonevanescent component, which belongs to

$$\mathbb{T}_{\leq N} := \bigoplus_{n=1}^{N} \mathbb{T}_n = \Big\{ \boldsymbol{A} \in L^2_t(S^2, \mathbb{C}^3) \;\Big|\; \boldsymbol{A} = \sum_{n=1}^{N} \boldsymbol{A}_n \,,\; \boldsymbol{A}_n \in \mathbb{T}_n \Big\}, \qquad N \gtrsim R \,,$$

for tangential far fields or $\mathbb{W}_{\leq N}$, $N \gtrsim R$, for normal far fields. Accordingly we aim to approximate the nonevanescent parts of solutions to the far field splitting and data completion problems only. This is a regularizing assumption, as we will see in Section 6 below.

5. Uncertainty principles

In this section we develop uncertainty principles[5] for the nonevanescent part of tangential far fields (i.e., far fields of electromagnetic waves and elastic shear waves), and we note that corresponding uncertainty principles for the nonevanescent part of normal far fields (i.e., far fields of elastic pressure waves) follow immediately from the scalar theory established in [8], because expansions in normal spherical harmonics can be reduced to scalar spherical harmonic expansions.

[5] These uncertainty principles have been motivated by similar results for the discrete and continuous one-dimensional Fourier transform in [3], and the corollaries in Section 6 are analogous to those in [3].

5.1. Uncertainty principles for far field splitting

In Section 4 we have restricted the discussion to sources supported in the ball $B_R(0)$ of radius R centered at the origin. If a source $\boldsymbol{F}$ is supported in a ball $B_R(\boldsymbol{c})$ with a different center $\boldsymbol{c} \neq 0$, we can shift it into $B_R(0)$ using the translation $\boldsymbol{F} \mapsto \boldsymbol{F}(\cdot + \boldsymbol{c})$. Since tangential far fields are projected restricted Fourier transforms, the formula for the Fourier transform of the translation of a function,

$$\widehat{\boldsymbol{F}(\cdot + \boldsymbol{c})}(\boldsymbol{\theta}) \;=\; e^{\mathrm{i}\boldsymbol{c}\cdot\boldsymbol{\theta}}\widehat{\boldsymbol{F}}(\boldsymbol{\theta})\,, \qquad \boldsymbol{\theta} \in S^2\,,\ \boldsymbol{c} \in \mathbb{R}^3\,,$$

can be used to describe the effect of this translation on the corresponding tangential far field. Accordingly, we call $T_{\boldsymbol{c}} : L_t^2(S^2, \mathbb{C}^3) \to L_t^2(S^2, \mathbb{C}^3)$ given by

$$(T_{\boldsymbol{c}}\boldsymbol{A})(\boldsymbol{\theta}) \;:=\; e^{\mathrm{i}\boldsymbol{c}\cdot\boldsymbol{\theta}}\boldsymbol{A}(\boldsymbol{\theta})\,, \qquad \boldsymbol{\theta} \in S^2\,, \tag{42}$$

the *far field translation operator* and note that $T_{\boldsymbol{c}}$ is unitary with $T_{\boldsymbol{c}}^* = T_{-\boldsymbol{c}}$.

Combining the Jacobi-Anger expansion

$$e^{\mathrm{i}\boldsymbol{c}\cdot\boldsymbol{\theta}} \;=\; \sum_{l=0}^{\infty} \mathrm{i}^l(2l+1)j_l(|\boldsymbol{c}|)P_l(\widehat{\boldsymbol{c}}\cdot\boldsymbol{\theta})\,, \qquad \boldsymbol{c} = |\boldsymbol{c}|\widehat{\boldsymbol{c}} \in \mathbb{R}^3\,,\ \boldsymbol{\theta}, \widehat{\boldsymbol{c}} \in S^2\,, \tag{43}$$

with the expansion (35) we obtain that

$$(T_{\boldsymbol{c}}\boldsymbol{A})(\boldsymbol{\theta}) \;=\; \sum_{n=1}^{\infty}\sum_{l=0}^{\infty} \mathrm{i}^l(2l+1)j_l(|\boldsymbol{c}|)P_l(\widehat{\boldsymbol{c}}\cdot\boldsymbol{\theta})\boldsymbol{A}_n(\boldsymbol{\theta})\,, \qquad \boldsymbol{\theta} \in S^2\,. \tag{44}$$

We denote by $\{\boldsymbol{A}_m^{\boldsymbol{c}}\}$ the vector spherical harmonic components of the translated field $T_{\boldsymbol{c}}\boldsymbol{A}$, and we also use $T_{\boldsymbol{c}}$ to denote the operator from $\ell^2(L_t^2(S^2, \mathbb{C}^3))$ to itself that operates directly on the vector spherical harmonic components $\{\boldsymbol{A}_n\}$ of $\boldsymbol{A}$ by

$$T_{\boldsymbol{c}}(\{\boldsymbol{A}_n\}) \;:=\; \{\boldsymbol{A}_m^{\boldsymbol{c}}\}\,. \tag{45}$$

The following notation will be a useful shorthand. Let $\boldsymbol{A} \in L_t^2(S^2, \mathbb{C}^3)$ with vector spherical harmonic coefficients $\{\boldsymbol{A}_n\}$, then

$$\|\boldsymbol{A}\|_{L^p} \;:=\; \Big(\int_{S^2} |\boldsymbol{A}(\boldsymbol{\theta})|^p \,\mathrm{d}s(\boldsymbol{\theta})\Big)^{\frac{1}{p}}, \quad 1 \le p < \infty\,, \qquad \|\boldsymbol{A}\|_{L^\infty} \;:=\; \operatorname*{ess\,sup}_{\boldsymbol{\theta}\in S^2} |\boldsymbol{A}(\boldsymbol{\theta})|\,, \tag{46a}$$

$$\|\boldsymbol{A}\|_{\ell^p} \;:=\; \Big(\sum_{n=1}^{\infty} \|\boldsymbol{A}_n\|_{L^2}^p\Big)^{\frac{1}{p}}, \quad 1 \le p < \infty\,, \qquad \|\boldsymbol{A}\|_{\ell^\infty} \;:=\; \sup_{n\ge 1} \|\boldsymbol{A}_n\|_{L^2}\,. \tag{46b}$$

The notation emphasizes that we treat the representation of the function $\boldsymbol{A}$ by its values, or by the sequence of its vector spherical harmonic components $\{\boldsymbol{A}_n\}$ as simply a way of inducing different norms. That is, both (46a) and (46b) describe different norms of the same tangential vector field on S^2. Because of the Parseval identity (38), $\|\boldsymbol{A}\|_{L^2} = \|\boldsymbol{A}\|_{\ell^2}$, so we may just write $\|\boldsymbol{A}\|_2$, and we write $\langle\cdot,\cdot\rangle$ for the corresponding inner product. We will even extend this notation a little more and refer to the support of $\boldsymbol{A}$ in S^2 as its L^0-support and denote by $\|\boldsymbol{A}\|_{L^0}$ the measure of $\operatorname{supp}\boldsymbol{A} \subseteq S^2$. Similarly, we will call the indices of the nonzero vector spherical harmonic components in the expansion (35) the ℓ^0-support of $\boldsymbol{A}$.

We will prove our uncertainty principles for far field translation, by showing that the far field translation operator is bounded on weighted ℓ^p spaces. Given any sequence of nonnegative weights $\{w_n\} \subseteq [0,\infty)$ we define

$$\ell^p_w(L^2_t(S^2,\mathbb{C}^3)) := \{\boldsymbol{A} \in L^2_t(S^2,\mathbb{C}^3) \mid \|\boldsymbol{A}\|_{\ell^p_w} < \infty\},$$

where

$$\|\boldsymbol{A}\|_{\ell^p_w} := \Big(\sum_{n=1}^{\infty} w_n \|\boldsymbol{A}_n\|_2^p\Big)^{\frac{1}{p}}, \quad 1 \le p < \infty, \qquad \|\boldsymbol{A}\|_{\ell^\infty_w} := \sup_{n\ge 1}(w_n\|\boldsymbol{A}_n\|_2).$$

The next theorem gives a lower bound on the angle between a nonevanescent tangential far field $\boldsymbol{A}$ and the translate $T_{\boldsymbol{c}}\boldsymbol{B}$ of a nonevanescent tangential far field $\boldsymbol{B}$ in terms of the ℓ^0-supports of $\boldsymbol{A}$ and $\boldsymbol{B}$ and the distance $|\boldsymbol{c}|$.

Theorem 5.1 (Uncertainty principle for far field translation)**.** *Let $\boldsymbol{A},\boldsymbol{B} \in L^2_t(S^2,\mathbb{C}^3)$ such that the corresponding vector spherical harmonic components $\{\boldsymbol{A}_n\}$ and $\{\boldsymbol{B}_n\}$ satisfy* $\operatorname{supp}\{\boldsymbol{A}_n\} \subseteq W_1$ *and* $\operatorname{supp}\{\boldsymbol{B}_n\} \subseteq W_2$ *with $W_1, W_2 \subseteq \mathbb{N}$, and let $\boldsymbol{c} \in \mathbb{R}^3$. Then,*

$$|\langle \boldsymbol{A}, T_{\boldsymbol{c}}\boldsymbol{B}\rangle|^2 \le \frac{\sum_{n\in W_1}(2n+1)^2 \sum_{n\in W_2}(2n+1)^2}{|\boldsymbol{c}|^{\frac{5}{3}}} \|\boldsymbol{A}\|_2^2 \|\boldsymbol{B}\|_2^2. \tag{47}$$

The proof of Theorem 5.1 is an immediate consequence of the following lemma.

Lemma 5.2. *Given $\boldsymbol{c} \in \mathbb{R}^3$ let $T_{\boldsymbol{c}}$ be the operator introduced in (42) and (45). Then, the operator norm of $T_{\boldsymbol{c}} : L^p_t(S^2,\mathbb{C}^3) \longrightarrow L^p_t(S^2,\mathbb{C}^3)$, $1 \le p \le \infty$, satisfies*

$$\|T_{\boldsymbol{c}}\|_{L^p,L^p} = 1, \tag{48}$$

whereas $T_{\boldsymbol{c}} : \ell^1_{2n+1} \longrightarrow \ell^\infty_{1/(2n+1)}$ satisfies

$$\|T_{\boldsymbol{c}}\|_{\ell^1_{2n+1},\ell^\infty_{1/(2n+1)}} \le \frac{1}{|\boldsymbol{c}|^{\frac{5}{6}}}. \tag{49}$$

Proof. The first estimate (48) is an immediate consequence of the definition (42).

Now let $\boldsymbol{A},\boldsymbol{B} \in L^2_t(S^2,\mathbb{C}^3)$ with vector spherical harmonic components $\{\boldsymbol{A}_n\},\{\boldsymbol{B}_n\}$, and denote by $\{\boldsymbol{A}^{\boldsymbol{c}}_n\}$ the vector spherical harmonic components of $T_{\boldsymbol{c}}\boldsymbol{A}$. Using (44) we find that, for any $m \ge 1$,

$$\begin{aligned}\langle \boldsymbol{B}_m, \boldsymbol{A}^{\boldsymbol{c}}_m\rangle &= \langle \boldsymbol{B}_m, T_{\boldsymbol{c}}\boldsymbol{A}\rangle \\ &= \sum_{n=1}^{\infty}\sum_{l=0}^{\infty} \mathrm{i}^l(2l+1)j_l(|\boldsymbol{c}|)\int_{S^2} P_l(\widehat{\boldsymbol{c}}\cdot\boldsymbol{\omega})\boldsymbol{A}_n(\boldsymbol{\omega})\cdot\overline{\boldsymbol{B}_m(\boldsymbol{\omega})}\,\mathrm{d}s(\boldsymbol{\omega}).\end{aligned} \tag{50}$$

The orthogonality relation in Corollary B.2 in Appendix B allows us to conclude that the interior sum in (50) is finite, and

$$\langle \boldsymbol{B}_m, \boldsymbol{A}^{\boldsymbol{c}}_m\rangle = \sum_{n=1}^{\infty}\sum_{l=|m-n|}^{m+n} \mathrm{i}^l(2l+1)j_l(|\boldsymbol{c}|)\int_{S^2} P_l(\widehat{\boldsymbol{c}}\cdot\boldsymbol{\omega})\boldsymbol{A}_n(\boldsymbol{\omega})\cdot\overline{\boldsymbol{B}_m(\boldsymbol{\omega})}\,\mathrm{d}s(\boldsymbol{\omega}).$$

Employing Hölder's inequality and then the bound on $\|P_l^{\widehat{\boldsymbol{c}}}\|_{L^\infty}$ from (33) gives,

$$\begin{aligned}|\langle \boldsymbol{B}_m, \boldsymbol{A}_m^{\boldsymbol{c}}\rangle| \;&\le\; \sum_{n=1}^{\infty} \|\boldsymbol{A}_n\|_2 \Big(\sum_{l=|m-n|}^{m+n} (2l+1)|j_l(|\boldsymbol{c}|)| \|P_l^{\widehat{\boldsymbol{c}}}\|_{L^\infty}\Big) \|\boldsymbol{B}_m\|_2 \\ &=\; \sum_{n=1}^{\infty} \|\boldsymbol{A}_n\|_2 \Big(\sum_{l=|m-n|}^{m+n} (2l+1)|j_l(|\boldsymbol{c}|)|\Big) \|\boldsymbol{B}_m\|_2 \,.\end{aligned}$$

Setting $\boldsymbol{B}_m = \boldsymbol{A}_m^{\boldsymbol{c}}$, we obtain, for any $m \ge 1$,

$$\|\boldsymbol{A}_m^{\boldsymbol{c}}\|_2 \;\le\; \sum_{n=1}^{\infty} \|\boldsymbol{A}_n\|_2 \Big(\sum_{l=|m-n|}^{m+n} (2l+1)|j_l(|\boldsymbol{c}|)|\Big) \,. \tag{51}$$

To estimate the term in parentheses, we recall that spherical Bessel functions satisfy

$$j_n(z) \;=\; \sqrt{\frac{\pi}{2z}} J_{n+\frac{1}{2}}(z)\,, \qquad z \in \mathbb{C}\,,\; n \in \mathbb{Z}\,, \tag{52}$$

where $J_{n+\frac{1}{2}}$ is a Bessel function, and employ the estimate of $J_{n+\frac{1}{2}}$ provided by the last inequality on page 199 of [19] to obtain

$$|j_n(|\boldsymbol{c}|)| \;<\; \frac{b_1}{|\boldsymbol{c}|^{\frac{5}{6}}} \qquad \text{with } b_1 \approx 0.9847\,. \tag{53}$$

Combining this estimate with the formula

$$\sum_{l=|m-n|}^{m+n} (2l+1) \;=\; (2m+1)(2n+1)$$

gives a further estimate for the right-hand side of (51),

$$\|\boldsymbol{A}_m^{\boldsymbol{c}}\|_2 \;\le\; (2m+1)\frac{1}{|\boldsymbol{c}|^{\frac{5}{6}}} \sum_{n=1}^{\infty} (2n+1)\|\boldsymbol{A}_n\|_2\,. \tag{54}$$

This implies that

$$\|T_{\boldsymbol{c}}\boldsymbol{A}\|_{\ell^\infty_{1/(2n+1)}} \;=\; \sup_{m\ge 1} \frac{\|\boldsymbol{A}_m^{\boldsymbol{c}}\|_2}{2m+1} \;\le\; \frac{1}{|\boldsymbol{c}|^{\frac{5}{6}}} \sum_{n=1}^{\infty} (2n+1)\|\boldsymbol{A}_n\|_2 \;=\; \frac{1}{|\boldsymbol{c}|^{\frac{5}{6}}} \|\boldsymbol{A}\|_{\ell^1_{2n+1}}\,.$$

□

Proof of Theorem 5.1. Hölder's inequality and (49) show that

$$\begin{aligned}|\langle \boldsymbol{A}, T_{\boldsymbol{c}}\boldsymbol{B}\rangle| \;&\le\; \sum_{n=1}^{\infty} |\langle \boldsymbol{A}_n, \boldsymbol{B}_n^{\boldsymbol{c}}\rangle| \;\le\; \|\boldsymbol{A}\|_{\ell^1_{2n+1}} \|T_{\boldsymbol{c}}\boldsymbol{B}\|_{\ell^\infty_{1/(2n+1)}} \;\le\; \frac{1}{|\boldsymbol{c}|^{\frac{5}{6}}} \|\boldsymbol{A}\|_{\ell^1_{2n+1}} \|\boldsymbol{B}\|_{\ell^1_{2n+1}} \\ &\le\; \frac{1}{|\boldsymbol{c}|^{\frac{5}{6}}} \Big(\sum_{n\in W_1} (2n+1)^2\Big)^{1/2} \|\boldsymbol{A}\|_2 \Big(\sum_{n\in W_2} (2n+1)^2\Big)^{1/2} \|\boldsymbol{B}\|_2\,.\end{aligned} \tag{55}$$

□

We will apply the uncertainty principle to the translates of the subspaces $\mathbb{T}_{\leq N}$ of nonevanescent tangential far fields radiated from $B_R(0)$, where N is just a little larger than R. For these subspaces, $W_1 = \{1 \ldots, N\}$, $W_2 = \{1 \ldots, M\}$, and we can improve the dependence on $|\boldsymbol{c}|$ in (47) under the hypothesis that $|\boldsymbol{c}|$ is a little more than twice as large as $M + N$. Geometrically, this means that the distance between two balls that support the far fields we wish to split is slightly greater than the sum of their diameters.

Theorem 5.3. *Suppose that $\boldsymbol{A} \in \mathbb{T}_{\leq N}$, $\boldsymbol{B} \in \mathbb{T}_{\leq M}$ with $M, N \geq 1$, and let $\boldsymbol{c} \in \mathbb{R}^3$ such that $|\boldsymbol{c}| > 2(M + N + \frac{3}{2})$. Then*

$$\begin{aligned} &|\langle \boldsymbol{A}, T_{\boldsymbol{c}} \boldsymbol{B} \rangle|^2 \\ &\leq\ b_2 \, \frac{((N+\frac{1}{2})(N+1)(N+\frac{3}{2})-1)((M+\frac{1}{2})(M+1)(M+\frac{3}{2})-1)}{|\boldsymbol{c}|^2} \|\boldsymbol{A}\|_2^2 \|\boldsymbol{B}\|_2^2 \end{aligned} \tag{56}$$

with $b_2 \approx 2.194$.

Proof of Theorem 5.3. Let $\boldsymbol{A} \in \mathbb{T}_{\leq N}$ with vector spherical harmonic components $\{\boldsymbol{A}_n\}$, and denote by $\{\boldsymbol{A}_n^{\boldsymbol{c}}\}$ the vector spherical harmonic components of $T_{\boldsymbol{c}}\boldsymbol{A}$. As in (54) we find that

$$\|\boldsymbol{A}_m^{\boldsymbol{c}}\|_2 \ \leq\ (2m+1) \sup_{0 \leq l \leq M+N} |j_l(|\boldsymbol{c}|)| \sum_{n=1}^{N} (2n+1) \|\boldsymbol{A}_n\|_2 \,.$$

Combining Theorem 2 of [15] with (52) it can be shown (see Appendix B in [8] for details) that

$$\sup_{0 \leq l \leq M+N} |j_l(|\boldsymbol{c}|)| \ \leq\ \frac{b_3}{|\boldsymbol{c}|} \qquad \text{with } b_3 \approx 1.111 \,, \tag{57}$$

and thus

$$\|T_{\boldsymbol{c}}\boldsymbol{A}\|_{\ell^\infty_{1/(2n+1)}} \ =\ \sup_{m \geq 1} \frac{\|\boldsymbol{A}_m^{\boldsymbol{c}}\|_2}{2m+1} \ \leq\ \frac{b_3}{|\boldsymbol{c}|} \sum_{n=1}^{\infty} (2n+1) \|\boldsymbol{A}_n\|_2 \ =\ \frac{b_3}{|\boldsymbol{c}|} \|\boldsymbol{A}\|_{\ell^1_{2n+1}} \,.$$

Now, proceeding as in (55) and using the formula

$$\sum_{n=1}^{N} (2n+1)^2 \ =\ \frac{4}{3}\Big(N+\frac{1}{2}\Big)(N+1)\Big(N+\frac{3}{2}\Big) - 1$$

yields (56). □

Its possible to prove a different version of an uncertainty principle for far field translation directly, without using the weighted ℓ^1-ℓ^∞ estimate from Lemma 5.2.[6]

Theorem 5.4. *Suppose that $\boldsymbol{A} \in \mathbb{T}_{\leq N}$, $\boldsymbol{B} \in \mathbb{T}_{\leq M}$ with $M, N \geq 1$, and let $\boldsymbol{c} \in \mathbb{R}^3$ such that $|\boldsymbol{c}| > 2(M + N + \frac{3}{2})$. Then*

$$|\langle \boldsymbol{A}, T_{\boldsymbol{c}} \boldsymbol{B} \rangle|^2 \ \leq\ b_3 \, \frac{(N+M+1)^4}{|\boldsymbol{c}|^2} \|\boldsymbol{A}\|_2^2 \|\boldsymbol{B}\|_2^2 \tag{58}$$

with $b_3 \approx 1.111$.

[6] Theorem 5.4 below and its proof were found by the anonymous referee of this paper

Proof. Corollary B.2 in Appendix B allows us to replace $e^{\mathrm{i}\boldsymbol{c}\cdot\boldsymbol{\theta}}$ in the following integral with a truncated Jacobi-Anger expansion (see (43)),

$$\begin{aligned}|\langle \boldsymbol{A}, T_{\boldsymbol{c}}\boldsymbol{B}\rangle| &= \Big|\int_{S^2} e^{\mathrm{i}\boldsymbol{c}\cdot\boldsymbol{\theta}}\,\overline{\boldsymbol{A}(\boldsymbol{\theta})}\cdot\boldsymbol{B}(\boldsymbol{\theta})\,\mathrm{d}s(\boldsymbol{\theta})\Big| \\ &= \Big|\int_{S^2}\Big(\sum_{l=0}^{M+N}\mathrm{i}^l(2l+1)j_l(|\boldsymbol{c}|)P_l(\widehat{\boldsymbol{c}}\cdot\boldsymbol{\theta})\Big)\overline{\boldsymbol{A}(\boldsymbol{\theta})}\cdot\boldsymbol{B}(\boldsymbol{\theta})\,\mathrm{d}s(\boldsymbol{\theta})\Big|\,.\end{aligned}$$

Using (57) to estimate the Bessel functions, and (33) to estimate the Legendre polynomials, we have

$$\begin{aligned}|\langle \boldsymbol{A}, T_{\boldsymbol{c}}\boldsymbol{B}\rangle| &\le \frac{b_3}{|\boldsymbol{c}|}\sup_{\boldsymbol{\theta}\in S^2}\Big|\sum_{l=0}^{M+N}\mathrm{i}^l(2l+1)P_l(\widehat{\boldsymbol{c}}\cdot\boldsymbol{\theta})\Big|\|\boldsymbol{A}\|_2\|\boldsymbol{B}\|_2 \\ &\le \frac{b_3}{|\boldsymbol{c}|}\sum_{l=0}^{M+N}(2l+1)\,\|\boldsymbol{A}\|_2\|\boldsymbol{B}\|_2 \;=\; \frac{b_3}{|\boldsymbol{c}|}\,(N+M+1)^2\,\|\boldsymbol{A}\|_2\|\boldsymbol{B}\|_2\,.\end{aligned}$$

□

Remark 5.5. For N and M of comparable size, (58) is stronger than (56), while the reverse is true if one of M or N is much larger than the other. Estimate (58) has the appealing physical interpretation that the angle between two far fields is bounded away from zero, and therefore the splitting of two far fields is well posed, if the source of each is in the Fraunhofer zone of the other.[7] More importantly, if we fix the geometry and vary the wavenumber, the constant in (58) is proportional to k^2 rather than k^3. This is consistent with similar estimates in two dimensions, and cannot be improved, as an example in [8, Sec. 6] for the scalar case shows. A slight modification of that example shows that the best we can hope for would be to replace $(N+M+1)^2$ in the inequality (58) by NM. The example shows that the cosine of the angle between the far field of a single layer source supported on a circlular plate with a diameter of W wavelengths, and the far field of its translate, is proportional to $\frac{W^2}{|\boldsymbol{c}|}$ if $|\boldsymbol{c}|$ and $|W|$ are large and $\frac{W^2}{|\boldsymbol{c}|}$ is small ($|\boldsymbol{c}|$ is also measured in wavelenghts) . If we instead choose the diameters of the two plates to be different, say W_1 and W_2, a similar calculation shows that the cosine of the angle is proportional to $\frac{W_1W_2}{|\boldsymbol{c}|}$ provided $\frac{(W_1+W_2)^2}{|\boldsymbol{c}|}$ is small. ◊

5.2. Uncertainty principles for data completion

We denote by $\mathcal{H} : L_t^2(S^2,\mathbb{C}^3) \to \ell^2(L_t^2(S^2,\mathbb{C}^3))$, $\mathcal{H}\boldsymbol{A} := \{\boldsymbol{A}_n\}$, the operator that maps a tangential vector field $\boldsymbol{A}$ on the unit sphere to its vector spherical harmonic components $\{\boldsymbol{A}_n\}$. Parseval's identity (38) implies that $\|\mathcal{H}\|_{2,2} = \|\mathcal{H}^{-1}\|_{2,2} = 1$. Furthermore, using the orthogonality of $\mathbb{U}_n$ and $\mathbb{V}_n$, it follows from (36) and (39) that,

[7] Again, thanks to the anonymous referee for this observation

for any $n \geq 1$,

$$\begin{aligned}
\|\boldsymbol{A}_n\|_{L^\infty}^2 &= \|\boldsymbol{A}_n^{(s)} + \boldsymbol{A}_n^{(t)}\|_{L^\infty}^2 \\
&= \Big(\frac{2n+1}{4\pi}\Big)^2 \Big\| \int_{S^2} (\boldsymbol{P}_n^{(s)} + \boldsymbol{P}_n^{(t)})(\boldsymbol{\theta}, \boldsymbol{\omega}) \boldsymbol{A}_n(\boldsymbol{\omega}) \, \mathrm{d}s(\boldsymbol{\omega}) \Big\|_{L^\infty}^2 \\
&\leq \Big(\frac{2n+1}{4\pi}\Big)^2 \sup_{\boldsymbol{\theta} \in S^2} \Big(\|\boldsymbol{P}_n^{(s,\boldsymbol{\theta})}\|_{L^2(S^2, \mathbb{C}^{3\times 3})}^2 \|\boldsymbol{A}_n^{(s)}\|_2^2 + \|\boldsymbol{P}_n^{(t,\boldsymbol{\theta})}\|_{L^2(S^2, \mathbb{C}^{3\times 3})}^2 \|\boldsymbol{A}_n^{(t)}\|_2^2 \Big) \\
&\leq \frac{2n+1}{4\pi} (\|\boldsymbol{A}_n^{(s)}\|_2^2 + \|\boldsymbol{A}_n^{(t)}\|_2^2) = \frac{2n+1}{4\pi} \|\boldsymbol{A}_n\|_2^2 .
\end{aligned}$$

Accordingly,

$$\|\boldsymbol{A}\|_{L^\infty} \leq \sum_{n=1}^{\infty} \|\boldsymbol{A}_n\|_{L^\infty} \leq \frac{1}{\sqrt{4\pi}} \sum_{n=1}^{\infty} \sqrt{2n+1} \|\boldsymbol{A}_n\|_2 = \frac{1}{\sqrt{4\pi}} \|\boldsymbol{A}\|_{\ell^1_{\sqrt{2n+1}}} , \tag{59}$$

and therefore, $\mathcal{H}^{-1} : \ell^1_{\sqrt{2n+1}}(L_t^2(S^2, \mathbb{C}^3)) \to L^\infty(S^2; \mathbb{C}^3)$ is bounded with

$$\|\mathcal{H}^{-1}\|_{\ell^1_{\sqrt{2n+1}}, L^\infty} \leq \frac{1}{\sqrt{4\pi}} .$$

The next theorem gives a lower bound on the angle between the translate $T_{\boldsymbol{c}}\boldsymbol{A}$ of a nonevanescent tangential far field $\boldsymbol{A}$ and a tangential vector field $\boldsymbol{B}$ supported only on part of S^2 in terms of the ℓ^0-support of $\boldsymbol{A}$ and the L^0-support of $\boldsymbol{B}$.

Theorem 5.6. *Let $\boldsymbol{A}, \boldsymbol{B} \in L_t^2(S^2, \mathbb{C}^3)$ such that the vector spherical harmonic components $\{\boldsymbol{A}_n\}$ of $\boldsymbol{A}$ satisfy $\operatorname{supp}\{\boldsymbol{A}_n\} \subseteq W$ with $W \subseteq \mathbb{N}$, and let $\boldsymbol{c} \in \mathbb{R}^3$. Then,*[8]

$$|\langle T_{\boldsymbol{c}}\boldsymbol{A}, \boldsymbol{B} \rangle|^2 \leq \frac{\|\boldsymbol{B}\|_{L^0}}{4\pi} \sum_{n \in W} (2n+1) \, \|\boldsymbol{A}\|_2^2 \|\boldsymbol{B}\|_2^2 .$$

Proof. Combining Hölder's inequality with (48) and (59) we find that

$$\begin{aligned}
|\langle T_{\boldsymbol{c}}\boldsymbol{A}, \boldsymbol{B} \rangle| &\leq \|T_{\boldsymbol{c}}\boldsymbol{A}\|_{L^\infty} \|\boldsymbol{B}\|_{L^1} \leq \|\boldsymbol{A}\|_{L^\infty} \|\boldsymbol{B}\|_{L^1} \leq \frac{1}{\sqrt{4\pi}} \sum_{n \in W} (\sqrt{2n+1} \|\boldsymbol{A}_n\|_2) \|\boldsymbol{B}\|_{L^1} \\
&\leq \frac{1}{\sqrt{4\pi}} \sqrt{\sum_{n \in W} (2n+1)} \|\boldsymbol{A}\|_2 \sqrt{\|\boldsymbol{B}\|_{L^0}} \|\boldsymbol{B}\|_2 .
\end{aligned}$$

□

For $\boldsymbol{A} \in \mathbb{T}_{\leq N}$, we may use the formula $\sum_{n=1}^{N} (2n+1) = (N+1)^2 - 1$ to restate Theorem 5.6 as follows.

Corollary 5.7. *Let $\boldsymbol{A} \in \mathbb{T}_{\leq N}$, $\boldsymbol{B} \in L_t^2(S^2, \mathbb{C}^3)$ with $\operatorname{supp} \boldsymbol{B} \subseteq \Omega \subseteq S^2$, and $\boldsymbol{c} \in \mathbb{R}^3$. Then*

$$|\langle T_{\boldsymbol{c}}\boldsymbol{A}, \boldsymbol{B} \rangle|^2 \leq \frac{|\Omega|}{4\pi} ((N+1)^2 - 1) \|\boldsymbol{A}\|_2^2 \|\boldsymbol{B}\|_2^2 .$$

[8] As before, $\|\boldsymbol{B}\|_{L^0}$ denotes the measure of $\operatorname{supp} \boldsymbol{B} \subseteq S^2$.

6. Stability estimates for far field splitting and data completion

The uncertainty principles developed in the previous section can be utilized to analyze the stability of numerical algorithms for far field splitting and data completion. In this section we discuss three applications of this kind for tangential far fields. Since, apart from the new uncertainty principles, the proofs of these results are similar to corresponding calculations for the scalar case in [7], we omit them here and refer the reader to [7] for proofs and additional applications of the uncertainty principles. We also note that corresponding results for normal far fields immediately follow from the three-dimensional scalar case considered in [8].

According to the regularized Picard criterion from Section 4.4, up to measurement precision p, a far field radiated by a limited power source with power threshold P in $B_R(0)$ coincides with a tangential vector field that belongs to the subspace of nonevanescent far fields $\mathbb{T}_{\leq N}$, where N is just a little bigger than R. Therefore, if we only consider the nonevanescent part, then the uncertainty principles from Theorems 5.3, 5.4, and Corollary 5.7 apply to this setting. Theorem 6.1 below gives conditions under which we can split the sum of two nonevanescent far fields radiated from well-separated localized sources into the original summands by solving a well-conditioned least squares problem, and provides a stability estimate.

Theorem 6.1. *Suppose that* $\boldsymbol{G}^0, \boldsymbol{G}^1 \in L^2_t(S^2, \mathbb{C}^3)$, $\boldsymbol{c}_1, \boldsymbol{c}_2 \in \mathbb{R}^3$, *and* $N_1, N_2 \in \mathbb{N}$ *such that*

$$|\boldsymbol{c}_1 - \boldsymbol{c}_2| \;>\; 2\Big(N_1 + N_2 + \frac{3}{2}\Big)$$

and

$$C \;:=\; b_2\,\frac{((N+\frac{1}{2})(N+1)(N+\frac{3}{2})-1)((M+\frac{1}{2})(M+1)(M+\frac{3}{2})-1)}{|\boldsymbol{c}_1-\boldsymbol{c}_2|^2} \;<\; 1 \tag{60}$$

with $b_2 \approx 2.194$ *or*

$$C \;:=\; b_3\,\frac{(M+N+1)^4}{|\boldsymbol{c}_1-\boldsymbol{c}_2|^2} \;<\; 1 \tag{61}$$

with $b_3 \approx 1.111$. *Let* $\boldsymbol{A}_i^j$ *be defined as least squares solutions to*

$$\boldsymbol{G}^0 \overset{\text{LS}}{=} T^*_{\boldsymbol{c}_1}\boldsymbol{A}_1^0 + T^*_{\boldsymbol{c}_2}\boldsymbol{A}_2^0\,, \qquad \boldsymbol{A}_i^0 \in \ell^2(\mathbb{T}_{\leq N_i})\,, \tag{62a}$$

$$\boldsymbol{G}^1 \overset{\text{LS}}{=} T^*_{\boldsymbol{c}_1}\boldsymbol{A}_1^1 + T^*_{\boldsymbol{c}_2}\boldsymbol{A}_2^1\,, \qquad \boldsymbol{A}_i^1 \in \ell^2(\mathbb{T}_{\leq N_i})\,. \tag{62b}$$

Then, for $i = 1, 2$,

$$\|\boldsymbol{A}_i^1 - \boldsymbol{A}_i^0\|_2^2 \;\leq\; (1-C)^{-1}\|\boldsymbol{G}^1 - \boldsymbol{G}^0\|_2^2\,. \tag{63}$$

A tangential far field $\boldsymbol{G}^j$ that is radiated by a limited power current source supported in $B_{R_1}(\boldsymbol{c}_1) \cup B_{R_2}(\boldsymbol{c}_2)$ will in general be very close to, but will not belong to the subspace $T^*_{\boldsymbol{c}_1} l^2(\mathbb{T}_{\leq N_1}) \oplus T^*_{\boldsymbol{c}_2} l^2(\mathbb{T}_{\leq N_2})$, with $N_i \gtrsim R_i$. Thus the tangential far fields $\boldsymbol{A}_1^j$ and $\boldsymbol{A}_2^j$ will usually not solve (62) exactly. However, the estimate (63) is always true and provides an explicit bound on the absolute condition number of the splitting operator, which maps $\boldsymbol{G}^j$ to $(\boldsymbol{A}_1^j, \boldsymbol{A}_2^j)$. The assumptions (60)–(61) essentially relates the radii R_i

of the balls which contain the supports of the sources and the distance $|\boldsymbol{c}_1 - \boldsymbol{c}_2|$ between their centers. Because we have normalized the wave number $k = 1$, it is necessary to multiply all distances by the actual wave number to return to physical units.

Next we consider a corresponding result for data completion. Assuming that a far field is radiated from a sufficiently small ball $B_R(\boldsymbol{c})$ and measured on a sufficiently large part of the sphere, Theorem 6.2 below says that its nonevanescent part can be recovered on the entire sphere by solving a well-conditioned least squares problem, and provides an explicit stability estimate. More precisely, we consider the case where the far field $\boldsymbol{A} = T_c^* \boldsymbol{A}^0$ cannot be measured on a subset $\Omega \subseteq S^2$, and instead we observe $\boldsymbol{G}^0 = \boldsymbol{A} + \boldsymbol{B}^0$, where $\boldsymbol{B}^0 = -\boldsymbol{A}|_\Omega$.

Theorem 6.2. *Suppose that* $\boldsymbol{G}^0, \boldsymbol{G}^1 \in L^2_t(S^2, \mathbb{C}^3)$, $\boldsymbol{c} \in \mathbb{R}^3$, $N \in \mathbb{N}$, *and* $\Omega \subseteq S^2$ *such that*

$$C := \frac{|\Omega|(N+1)^2}{4\pi} < 1\,, \tag{64}$$

and let $\boldsymbol{B}^i$ *and* $\boldsymbol{A}^i$ *be defined as the least squares solutions to*

$$\begin{aligned} \boldsymbol{G}^0 &\overset{\text{LS}}{=} \boldsymbol{B}^0 + T_{\boldsymbol{c}}^* \boldsymbol{A}^0\,, \qquad \boldsymbol{A}^0 \in \ell^2(\mathbb{T}_{\le N}) \text{ and } \boldsymbol{B}^0 \in L^2(\Omega, \mathbb{C}^3)\,, \\ \boldsymbol{G}^1 &\overset{\text{LS}}{=} \boldsymbol{B}^1 + T_{\boldsymbol{c}}^* \boldsymbol{A}^1\,, \qquad \boldsymbol{A}^1 \in \ell^2(\mathbb{T}_{\le N}) \text{ and } \boldsymbol{B}^1 \in L^2(\Omega, \mathbb{C}^3)\,. \end{aligned}$$

Then

$$\|\boldsymbol{A}^1 - \boldsymbol{A}^0\|_2^2 \le (1-C)^{-1} \|\boldsymbol{G}^1 - \boldsymbol{G}^0\|_2^2\,,$$

$$\|\boldsymbol{B}^1 - \boldsymbol{B}^0\|_2^2 \le (1-C)^{-1} \|\boldsymbol{G}^1 - \boldsymbol{G}^0\|_2^2\,.$$

The assumption (64) relates the radius R (again, in wavelenghts) of the support of the source and the area $|\Omega|$ of the missing data segment.

Finally, we note that the results of Theorem 6.1 can be extended to multiple well-separated components and that far field splitting and data completion can actually be combined (just as in the two-dimensional scalar case in Theorem 5.7 of [7]). Because the sum of the radii of the supports of well-separated localized source components may be much less than the radius of a large ball that contains them all, combining data completion with splitting as in Theorem 6.3 below may significantly improve the conditioning of the data completion problem.

Theorem 6.3. *Suppose that* $\boldsymbol{G}^0, \boldsymbol{G}^1 \in L^2_t(S^2, \mathbb{C}^3)$, $\boldsymbol{c}_i \in \mathbb{R}^3$, $N_i \in \mathbb{N}$, $i = 1, \dots, I$, *and* $\Omega \subseteq S^2$ *such that, for every* $i \ne j$, $|\boldsymbol{c}_i - \boldsymbol{c}_j| > 2(N_i + N_j + \frac{3}{2})$, *and that, for each* i,

$$\begin{aligned} C_{\boldsymbol{A},i} &:= \sqrt{\frac{|\Omega|}{4\pi}}(N_i+1) \\ &+ \sqrt{b_2}\sqrt{\Big(N_i+\frac{1}{2}\Big)(N_i+1)\Big(N_i+\frac{3}{2}\Big) - 1} \sum_{j \ne i} \frac{\sqrt{\Big(N_j+\frac{1}{2}\Big)(N_j+1)\Big(N_j+\frac{3}{2}\Big) - 1}}{|\boldsymbol{c}_i - \boldsymbol{c}_j|} < 1 \end{aligned} \tag{66a}$$

with $b_2 \approx 2.194$ *or*

$$C_{\boldsymbol{A},i} := \sqrt{\frac{|\Omega|}{4\pi}}(N_i+1) + \sqrt{b_3} \sum_{j \ne i} \frac{(N_i+N_j+1)^2}{|\boldsymbol{c}_i - \boldsymbol{c}_j|} < 1 \tag{66b}$$

with $b_3 \approx 1.111$. *Assume also that,*

$$C_{\boldsymbol{B}} := \sqrt{\frac{|\Omega|}{4\pi}} \sum_{i=1}^{I} (N_i + 1) < 1 \,. \tag{66c}$$

Let $\boldsymbol{A}_i^j$ *and* $\boldsymbol{B}^j$ *be defined as the least squares solutions to*

$$\boldsymbol{G}^0 \overset{LS}{=} \boldsymbol{B}^0 + \sum_{i=1}^{I} T_{\boldsymbol{c}_i}^* \boldsymbol{A}_i^0 \,, \qquad \boldsymbol{A}_i^0 \in \ell^2(\mathbb{T}_{\leq N_i}) \text{ and } \boldsymbol{B}^0 \in L^2(\Omega, \mathbb{C}^3) \,, \tag{67a}$$

$$\boldsymbol{G}^1 \overset{LS}{=} \boldsymbol{B}^1 + \sum_{i=1}^{I} T_{\boldsymbol{c}_i}^* \boldsymbol{A}_i^1 \,, \qquad \boldsymbol{A}_i^1 \in \ell^2(\mathbb{T}_{\leq N_i}) \text{ and } \boldsymbol{B}^1 \in L^2(\Omega, \mathbb{C}^3) \,. \tag{67b}$$

Then, for $i = 1, \ldots, I$,

$$\|\boldsymbol{A}_i^1 - \boldsymbol{A}_i^0\|_2^2 \leq (1 - C_{\boldsymbol{A},i})^{-1} \|\boldsymbol{G}^1 - \boldsymbol{G}^0\|_2^2 \,,$$

$$\|\boldsymbol{B}^1 - \boldsymbol{B}^0\|_2^2 \leq (1 - C_{\boldsymbol{B}})^{-1} \|\boldsymbol{G}^1 - \boldsymbol{G}^0\|_2^2 \,.$$

7. A numerical example

To illustrate our theoretical findings, we briefly describe a numerical implementation of the least squares formulation for simultaneous data completion and far field splitting as considered in Theorem 6.3. Again we restrict the discussion to tangential far fields, and note that normal far fields can be treated in exactly the same way that three-dimensional scalar far fields where treated in [8]. The algorithm is an extension of methods described in [5, 7, 8].

Let $\boldsymbol{A} = \sum_{i=1}^{I} T_{\boldsymbol{c}_i}^* \boldsymbol{A}_i$ denote a far field that is a superposition of far fields $T_{\boldsymbol{c}_i}^* \boldsymbol{A}_i$ radiated by limited power sources supported in balls $B_{R_i}(\boldsymbol{c}_i)$, for some $\boldsymbol{c}_i \in \mathbb{R}^3$ and $R_i > 0$. We suppose that we are able to measure $\boldsymbol{A}$ on $S^2 \setminus \Omega$. In addition, we suppose that we have a priori information on the approximate locations of the supports of the individual source components, i.e., $B_{R_i}(\boldsymbol{c}_i)$, $i = 1, \ldots, I$. Our aim is to reconstruct the nonevanescent part of $\boldsymbol{A}|_\Omega$ from $\boldsymbol{A}|_{S^2 \setminus \Omega}$. If we write $\boldsymbol{G} := \boldsymbol{A}|_{S^2 \setminus \Omega}$ for the observed far field data and $\boldsymbol{B} := -\boldsymbol{A}|_\Omega$, then

$$\boldsymbol{G} = \boldsymbol{B} + \sum_{i=1}^{I} T_{\boldsymbol{c}_i}^* \boldsymbol{A}_i \,,$$

i.e., we are in the framework of Theorem 6.3.

To formulate the least squares problem, we introduce the short hand notation

$$V_0 := L_t^2(\Omega, \mathbb{C}^3) := \{\boldsymbol{u} \in L^2(\Omega, \mathbb{C}^3) \mid \boldsymbol{\nu} \cdot \boldsymbol{u} = 0 \text{ a.e. on } S^2\}$$

and $V_i := T_{\boldsymbol{c}_i}^* \ell^2(\mathbb{T}_{\leq N_i})$, $i = 1, \ldots, I$, and let $P_0, \ldots, P_I$ denote the orthogonal projections onto $V_0, \ldots, V_I$, respectively. Then (67) is equivalent to seeking approximations $\boldsymbol{a}_i \in V_i$

of $T^*_{\boldsymbol{c}_i}\boldsymbol{A}_i$, $i = 1, \ldots, I$, and $\boldsymbol{b} \in V_0$ of $\boldsymbol{B}$ satisfying the system of linear equations

$$\begin{pmatrix} I & P_0P_1 & \cdots & P_0P_I \\ P_1P_0 & I & \cdots & P_1P_I \\ \vdots & \vdots & & \vdots \\ P_IP_0 & P_IP_1 & \cdots & I \end{pmatrix} \begin{pmatrix} \boldsymbol{b} \\ \boldsymbol{a}_1 \\ \vdots \\ \boldsymbol{a}_I \end{pmatrix} = \begin{pmatrix} 0 \\ P_1\boldsymbol{G} \\ \vdots \\ P_I\boldsymbol{G} \end{pmatrix}. \tag{68}$$

We choose the numbers $N_1, \ldots, N_I$ that determine the dimension of the individual subspaces $V_1, \ldots, V_I$ subject to the regularized Picard criterion from Section 4.4, i.e., such that $N_i \gtrsim kR_i$. The stability result in Theorem 6.3 gives an upper bound on the absolute condition number of the block-operator on the left-hand side of (68).

Assuming that the whole collection of sources is contained in a ball $B_R(0)$ of radius $R > 0$ around the origin, the nonevanescent part of $\boldsymbol{A}$ (and of each far field component $T^*_{c_1}\boldsymbol{A}_1, \ldots, T^*_{\boldsymbol{c}_I}\boldsymbol{A}_I$) is well approximated by its orthogonal projection onto the subspace $\mathbb{T}_{\leq N} \subseteq L^2_t(S^2, \mathbb{C}^3)$ with $N \gtrsim kR$. In our numerical implementation we approximate a solution of the restriction of (68) to this finite dimensional subspace.

From the proofs of Theorems 6.1 and 6.2 we immediately find that the square roots of the left-hand sides of (60) and (64) constitute upper bounds on the operator norms $\|P_iP_j\|_{2,2}$ of the entries of the block-operator on the left-hand side of (68). Accordingly, if (66) is satisfied, then this self-adjoint block-operator is strictly diagonally dominant, and thus positive definite. Hence, we apply the conjugate gradient method to solve the restriction of the linear system (68) to $\mathbb{T}_{\leq N}$, evaluating the projections P_iP_j in each iteration using discrete vector spherical harmonic transforms.

To evaluate these discrete vector spherical harmonic transforms, i.e., the vector spherical harmonic components of a tangential vector field $\boldsymbol{C} \in \mathbb{T}_{\leq N}$, we work in spherical coordinates,

$$\boldsymbol{\theta}(\vartheta, \varphi) = (\cos\varphi \sin\vartheta, \sin\varphi \sin\vartheta, \cos\vartheta), \qquad \vartheta \in [0, \pi], \ \varphi \in [0, 2\pi),$$

and consider the usual orthonormal basis of $\mathbb{Y}_n$, $n \in \mathbb{N}$, that is given by

$$Y^m_n(\vartheta, \varphi) := C^m_n P^{|m|}_n(\cos\vartheta) e^{\mathrm{i}m\varphi}, \qquad -n \leq m \leq n,$$

where $C^m_n := \sqrt{\frac{2n+1}{4\pi}\frac{(n-|m|)!}{(n+|m|)!}}$ and $P^{|m|}_n$ denotes the associated Legendre functions (see, e.g., [2, p. 26]). Accordingly, evaluating the surface derivatives in (23), we find that orthonormal bases of $\mathbb{U}_n$ and $\mathbb{V}_n$, $n \geq 1$, are given by

$$\boldsymbol{U}^m_n(\vartheta, \varphi) = \frac{1}{\sin\vartheta}\frac{C^m_n}{\sqrt{n(n+1)}}\Big(-\sin^2(\vartheta)(P^{|m|}_n)'(\cos\vartheta)\boldsymbol{e}_\vartheta e^{\mathrm{i}m\varphi} + \mathrm{i}mP^{|m|}_n(\cos\vartheta)\boldsymbol{e}_\varphi e^{\mathrm{i}m\varphi}\Big)$$

and

$$\boldsymbol{V}^m_n(\vartheta, \varphi) = \frac{1}{\sin\vartheta}\frac{C^m_n}{\sqrt{n(n+1)}}\Big(-\sin^2(\vartheta)(P^{|m|}_n)'(\cos\vartheta)\boldsymbol{e}_\varphi e^{\mathrm{i}m\varphi} - \mathrm{i}mP^{|m|}_n(\cos\vartheta)\boldsymbol{e}_\vartheta e^{\mathrm{i}m\varphi}\Big),$$

$-n \leq m \leq n$, with $\boldsymbol{e}_\vartheta := (\cos\vartheta\cos\varphi, \cos\vartheta\sin\varphi, -\sin\varphi)$ and $\boldsymbol{e}_\varphi := (-\sin\varphi, \cos\varphi, 0)$. The derivative of the associated Legendre functions can rewritten using formula (14.10.5) in [21] to obtain

$$-\sin^2(\vartheta)(P^{|m|}_n)'(\cos\vartheta) = n\cos\vartheta P^{|m|}_n(\cos\vartheta) - (n + |m|)P^{|m|}_{n-1}(\cos\vartheta).$$

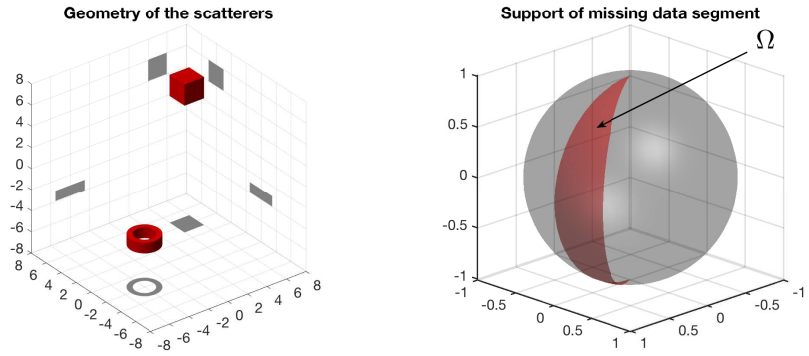

Figure 1. Left: Geometry of scatterers. Right: Support of missing data segment.

Then, the vector spherical harmonic components $\boldsymbol{C}_n = \boldsymbol{C}_n^{(t)} + \boldsymbol{C}_n^{(s)} \in \mathbb{T}_n$, $n \geq 1$, of $\boldsymbol{C}$ are given by

$$\boldsymbol{C}_n^{(t)} = \sum_{m=-n}^{n} \langle \boldsymbol{U}_n^m, \boldsymbol{C} \rangle \boldsymbol{U}_n^m \qquad \text{and} \qquad \boldsymbol{C}_n^{(s)} = \sum_{m=-n}^{n} \langle \boldsymbol{V}_n^m, \boldsymbol{C} \rangle \boldsymbol{V}_n^m \,. \tag{69}$$

We approximate the scalar products in (69) using the trapezoid rule with uniform spacing for the integral over φ, and Gauss-Legendre quadrature with respect to the variable $\zeta = \cos\vartheta$, $-1 \leq \zeta \leq 1$, for the integral over ϑ (see, e.g., [1, Sect. 5.1]). Accordingly, we suppose in our numerical example below that far field data are available on a grid

$$\Theta := \{\boldsymbol{\theta}(\vartheta_l, \varphi_m) \,|\, \vartheta_l = \sqrt{1-\zeta_l^2},\ \varphi_m = m\pi/M,\ l = 1, \ldots, M,\ m = 0, \ldots, 2M-1\}, \tag{70}$$

where $\zeta_1, \ldots, \zeta_M$ denote the Gauss-Legendre quadrature nodes on $[-1, 1]$. Since we have assumed that $\boldsymbol{C} \in \mathbb{T}_{\leq N}$, Corollary B.2 in Appendix B shows that the integrands in (69) belong to $\mathbb{T}_{\leq 2N}$ for $1 \leq n \leq N$, and following [1, Thm. 5.4], it is therefore appropriate to choose $M \geq N + 1$.

Example 7.1. We consider an electromagnetic scattering problem with two obstacles as shown in Figure 1 (left), which are illuminated by an incident plane wave $\boldsymbol{E}^i(\boldsymbol{x}) = \boldsymbol{p}e^{\mathrm{i}k\boldsymbol{x}\cdot\boldsymbol{d}}$, $\boldsymbol{x} \in \mathbb{R}^3$, with incident direction $\boldsymbol{d} = (1, 0, 0)$, polarization vector $\boldsymbol{p} = (0, 0, 1)$, and wave number $k = 5$ (i.e., the wavelength is $\lambda = 2\pi/5 \approx 1.26$). For better visualization this plot shows the projections of the scatterers on the three coordinate planes. The diameters of the two obstacles (in conventional units) are 3.16 (torus) and 3.46 (cube), and both of them are contained in the ball $B_{10}(0)$ of radius $R = 10$ around the origin. Accordingly, we choose $N = 60$ (i.e., $N \gtrsim kR$).

Assuming that the scatterers are perfectly conducting, the scattered field $\boldsymbol{E}^s$ satisfies the homogeneous Maxwell system outside the obstacles, the Silver-Müller radiation condition at infinity, and boundary condition $\boldsymbol{\nu} \times \boldsymbol{E}^s = 0$ on the boundaries of the obstacles. We simulate the far field $\boldsymbol{A}$ of the scattered field on the grid $\Theta \subseteq S^2$

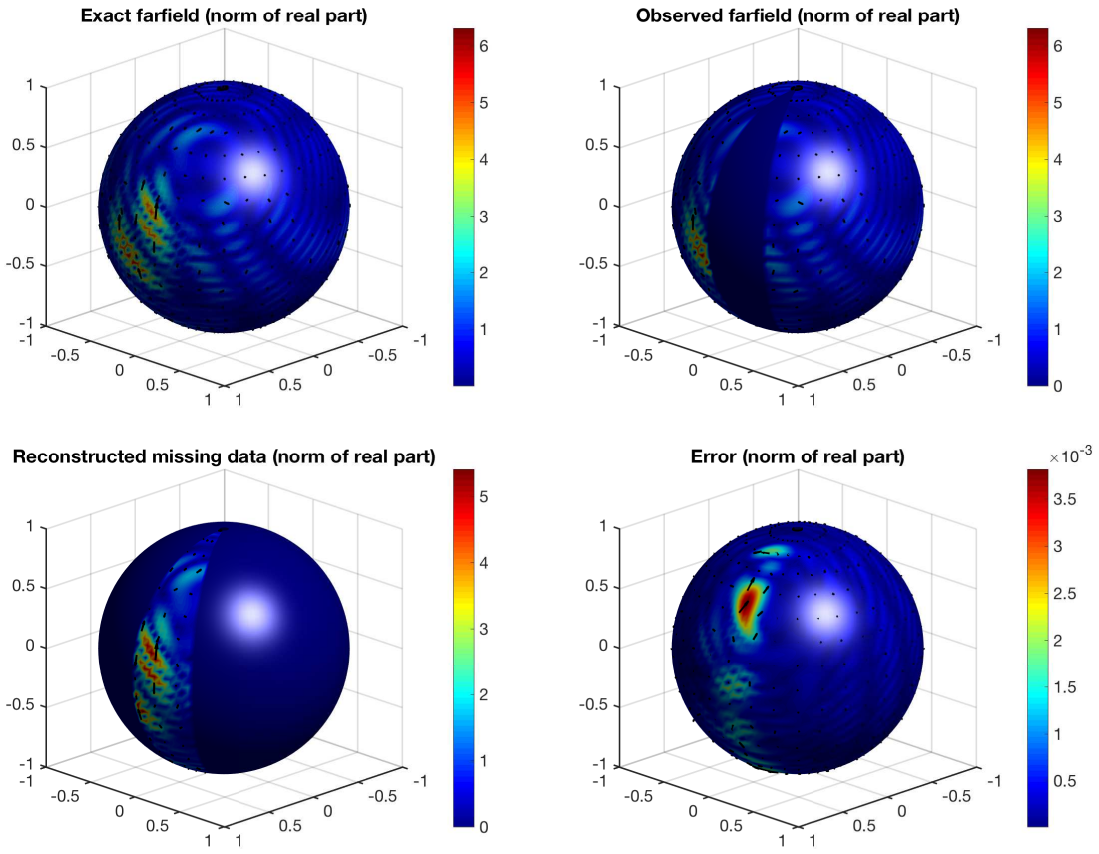

Figure 2. Top left: Norm of real part of exact far field $\boldsymbol{A}$. Top right: Norm of real part of observed far field $\boldsymbol{G}$. Bottom left: Norm of real part of reconstruction of missing data segment $\boldsymbol{A}|_\Omega$. Bottom right: Norm of real part of difference between exact and reconstructed far field on whole sphere.

from (70) with $M = 64$ (i.e., $M \gtrsim N + 1$) using a boundary element method.[9]

Figure 2 (top left) shows a visualization of the norm of the real part of $\boldsymbol{A}$ over the sphere. Since this far field $\boldsymbol{A}$ can immediately be rewritten as a superposition of two far fields radiated by two individual smooth volume sources supported in arbitrarily small neighborhoods of the scattering obstacles (cf., e.g., [17, Lemma 3.6]), this example actually fits into the framework of the previous sections. We consider this example as an instance of a far field radiated by two highly non-trivial compactly supported volume sources.

We suppose that the far field cannot be measured on the segment

$$\Omega = \{\boldsymbol{\theta}(\vartheta, \varphi)) \mid 0 \leq \vartheta \leq \pi\,,\ 0 < \varphi < \pi/6\} \subseteq S^2\,,$$

illustrated in Figure 1 (right), which has area $|\Omega| = \pi/3$. We assume a priori that the supports of the individual source components are contained in the balls $B_{R_i}(\boldsymbol{c}_i)$, $i = 1, 2$, with $\boldsymbol{c}_1 = (5, 4, 5)$, $\boldsymbol{c}_2 = (-4, -2, -4)$ and $R_1 = 2$, $R_2 = 2$, and we choose $N_1 = 14$ (i.e.,

[9] The data have been generated using the C++ boundary element library BEM++ (see [24, 25]).

$N_1 \gtrsim kR_1$) and $N_2 = 14$ (i.e., $N_2 \gtrsim kR_2$), and solve the linear system (68), restricted to $\mathbb{T}_{\leq N}$, using 500 conjugate gradient iterations. Figure 2 shows plots of the (pointwise Euclidean) norm of the real part of the observed data $\boldsymbol{G}$ (top right), the norm of the real part of the reconstruction of the missing data segment (bottom left), and the norm of the real part of the difference between the exact far field and the reconstructed far field on the whole sphere (bottom right).

The relative approximation error of this reconstruction is

$$\frac{\|\boldsymbol{A}|_\Omega + \boldsymbol{b}\|_{L^2(\Omega)}}{\|\boldsymbol{A}|_\Omega\|_{L^2(\Omega)}} \approx 7.531 \cdot 10^{-4} \qquad \text{and} \qquad \frac{\|\boldsymbol{A} - (\boldsymbol{a}_1 + \boldsymbol{a}_2)\|_2}{\|\boldsymbol{A}\|_2} \approx 4.889 \cdot 10^{-4}\,.$$

To put this into perspective, we note that the best approximation error of the simulated far field data $\boldsymbol{A}$ in $\mathbb{T}_{\leq N}$ satisfies

$$\frac{\|\boldsymbol{A} - (\boldsymbol{\mathcal{P}}_N^{(s)} + \boldsymbol{\mathcal{P}}_N^{(t)})\boldsymbol{A}\|_2}{\|\boldsymbol{A}\|_2} \approx 1.454 \cdot 10^{-4}\,.$$

Conclusions

Accurately locating and estimating the size of sources and scatterers based on far field observations is a basic problem in remote sensing. The cosine of the angle between the spaces of nonevanescent far fields indicates how far apart sources and scatterers must be before we can distinguish them from remote observations. Similarly, the cosine of the angle between fields supported in a compact subset of the sphere and nonevanescent far fields indicates how large an area of the sphere must be covered by sensors in order to guarantee that the far field can be reconstructed with a reasonable condition number from fixed frequency observations. Both of these questions can be rephrased as splitting problems, and the corresponding cosines can be (in some cases sharply) estimated by uncertainty principles. In this work we have shown how to extend scalar uncertainty principles to uncertainty principles for vector-valued far fields, in particular, those far fields radiated by time harmonic current sources modelled by Maxwell's equations, and to the far fields of elastic waves modelled by the Navier equations for a homogeneous medium. Along the way we have shown that the analysis of both the Maxwell and the Navier systems can be derived from the analysis of the vector Helmholtz equation in a straightforward way, and therefore that the far fields radiated by sources in either cases are tangential or normal components of restricted Fourier transforms.

Acknowledgments

The research of J.S. was supported in part by NSF grant DMS–1712525. We are grateful to the anonymous referee of this paper for sharing the results in Theorem 5.4 and Remark A.5 with us.

A. Properties of the rescaled squared singular values

We provide proofs for the qualitative properties of the rescaled squared singular values $r_n^2(R)$ and $t_n^2(R)$ of the tangential and normal restricted Fourier transform as stated in Remarks 4.1 and 4.2. The corresponding characteristics of the rescaled squared singular values $s_n^2(R)$ of the tangential restricted Fourier transform from Remark 4.1 have been shown in [8], and our proofs build on these results.

As in (28) and (30) we define the numbers $r_n^2(R)$, $s_n^2(R)$, and $t_n^2(R)$ for $n \geq 0$ by

$$r_n^2(R) := 4\pi \int_0^R (n(n+1)j_n^2(r) + (j_n(r) + rj_n'(r))^2) \, \mathrm{d}r \,, \tag{A.1a}$$

$$s_n^2(R) := 4\pi \int_0^R j_n^2(r) r^2 \, \mathrm{d}r \,, \tag{A.1b}$$

$$t_n^2(R) := 4\pi \int_0^R (n(n+1)j_n^2(r) + (rj_n'(r))^2) \, \mathrm{d}r \,. \tag{A.1c}$$

Integrating by parts and using the spherical Bessel equation shows that

$$t_n^2(R) = s_n^2(R) + 2\pi R^2 (j_n^2)'(R) \,, \tag{A.2a}$$

$$r_n^2(R) = t_n^2(R) + 4\pi R j_n^2(R) \,. \tag{A.2b}$$

Lemma A.1.

$$\sum_{n=0}^{\infty} (2n+1) r_n^2(R) = \frac{4\pi}{3} R^3 + 4\pi R \,, \quad \sum_{n=0}^{\infty} (2n+1) s_n^2(R) = \sum_{n=0}^{\infty} (2n+1) t_n^2(R) = \frac{4\pi}{3} R^3 \,.$$

Proof. We have already shown in Lemma A.1 of [8] that

$$\sum_{n=0}^{\infty} (2n+1) s_n^2(R) = \frac{4\pi}{3} R^3 \,.$$

Using formula 10.60.12 of [21], which implies that

$$\sum_{n=0}^{\infty} (2n+1)(j_n^2)'(R) = \Big(\sum_{n=0}^{\infty} (2n+1) j_n^2 \Big)'(R) = 0 \,,$$

the results follow from (A.2). □

Next we show that even and odd rescaled squared singular values, $s_n^2(R)$, $r_n^2(R)$, and $t_n^2(R)$, are monotonically decreasing as functions of n.

Lemma A.2. *For any $n \geq 1$,*

$$r_{n-1}^2(R) \geq r_{n+1}^2(R) \,, \quad s_{n-1}^2(R) \geq s_{n+1}^2(R) \,, \quad \textit{and} \quad t_{n-1}^2(R) \geq t_{n+1}^2(R) \,.$$

Proof. It has been shown in the proof of Lemma A.2 of [8] that

$$s_{n-1}^2(R) - s_{n+1}^2(R) = 4\pi(2n+1) R j_n^2(R) \geq 0 \,.$$

Using recurrence relations for Bessel functions (cf. [21, 10.51.1, 10.51.2]) we find that

$$j_{n-1}(R) j_{n-1}'(R) - j_{n+1}(R) j_{n+1}'(R) = \frac{n-1}{R} j_{n-1}^2(R) + \frac{n+2}{R} j_{n+1}^2(R) - \frac{2n+1}{R} j_n^2(R) \,.$$

Accordingly, (A.2) implies that

$$t_{n-1}^2(R) - t_{n+1}^2(R) \;=\; 4\pi R^2\Big(\frac{n-1}{R} j_{n-1}^2(R) + \frac{n+2}{R} j_{n+1}^2(R)\Big) \;\geq\; 0$$

and

$$r_{n-1}^2(R) - r_{n+1}^2(R) \;=\; 4\pi R\Big(n j_{n-1}^2(R) + (n+1) j_{n+1}^2(R)\Big) \;\geq\; 0\,.$$

□

When $n \geq R$, then the rescaled squared singular values, $s_n^2(R)$, $r_n^2(R)$ and $t_n^2(R)$, are strictly monotonically decreasing as functions of n.

Lemma A.3. *For any $n \in \mathbb{N}$ with $\sqrt{(n-1)n} \geq R > 0$,*

$$r_{n-1}^2(R) \;>\; r_n^2(R)\,, \quad s_{n-1}^2(R) \;>\; s_n^2(R) \quad \textit{and} \quad t_{n-1}^2(R) \;>\; t_n^2(R)\,.$$

Proof. Integrating the spherical Bessel equation from 0 to R, we find that

$$\int_0^R (n(n+1) - r^2) j_n(r)\, \mathrm{d}r \;=\; R^2 j_n'(R)\,. \tag{A.3}$$

Since

$$j_n(z) \;=\; \sqrt{\frac{\pi}{2z}} J_{n+\frac{1}{2}}(z)\,, \qquad z \in \mathbb{C}\,,\; n \in \mathbb{Z}\,, \tag{A.4}$$

we obtain from [21, 10.14.7, 10.14.2] that

$$j_n(r) \;=\; \sqrt{\frac{\pi}{2r}} J_\nu(r) \;\geq\; \sqrt{\frac{\pi}{2r}} \Big(\frac{r}{\nu}\Big)^\nu J_\nu(\nu) \;>\; 0\,, \qquad 0 < r \leq \nu := n + \frac{1}{2}\,.$$

Thus, if $(n+1)n \geq R^2$, then the integrand in (A.3) is nonnegative, and therefore

$$j_n'(r) \;>\; 0\,, \qquad 0 < r \leq \sqrt{(n+1)n}\,.$$

Using the recurrence relations [21, 10.51.1], this implies that

$$n j_{n-1}(r) - (n+1) j_{n+1}(r) \;=\; (2n+1) j_n'(r) \;>\; 0\,, \qquad 0 < r < \sqrt{(n+1)n}\,,$$

and applying [21, 10.51.1] once more, we obtain that, for $0 < r \leq \sqrt{(n+1)n}$,

$$j_n(r) \;=\; \frac{r}{2n+1}(j_{n-1}(r) + j_{n+1}(r)) \;<\; \frac{r}{n+1} j_{n-1}(r) \;<\; j_{n-1}(r)\,. \tag{A.5}$$

Accordingly,

$$s_n^2(R) \;=\; 4\pi \int_0^R j_n^2(r) r^2\, \mathrm{d}r \;<\; 4\pi \int_0^R j_{n-1}^2(r) r^2\, \mathrm{d}r \;<\; s_{n-1}^2(R)\,, \quad 0 < R \leq \sqrt{(n+1)n}\,.$$

Using the recurrence relations [21, 10.51.2], we find that, for $0 < r \leq \sqrt{n(n-1)}$,

$$j_n'(r) \;=\; \frac{n+1}{r} j_{n-1}'(r) - \frac{(n^2-1) - r^2}{r^2} j_{n-1}(r) \;<\; \frac{n+1}{r} j_{n-1}'(r)\,, \tag{A.6}$$

and combining (A.5) and (A.6) shows that

$$j_n(r) j_n'(r) \;<\; j_{n-1}(r) j_{n-1}'(r)\,, \qquad 0 < r \leq \sqrt{n(n-1)}\,.$$

Therefore, for $0 < R \leq \sqrt{n(n-1)}$,

$$t_n^2(R) \,=\, s_n^2(R) + 4\pi R^2 j_n(R) j_n'(R) \,<\, s_{n-1}^2(R) + 4\pi R^2 j_{n-1}(R) j_{n-1}'(R) \,=\, t_{n-1}^2(R)$$

and

$$r_n^2(R) \,=\, t_n^2(R) + 4\pi R j_n^2(R) \,<\, t_{n-1}^2(R) + 4\pi R j_{n-1}^2(R) \,=\, r_{n-1}^2(R)\,.$$

□

Next we provide upper bounds for $r_n^2(R)$, $s_n^2(R)$, and $t_n^2(R)$ when $n \geq R$.

Lemma A.4. *Suppose that $n \geq R > 0$. Then*

$$r_n^2(R) \,\leq\, b_0\Big(3\sqrt{e}\max\Big\{1, \frac{1}{R}\Big\} + R + \frac{2\sqrt{e}}{R}\Big)\Big(n+\frac{3}{2}\Big)^{\frac{2}{3}}\Big(\frac{R^2}{n^2}e^{1-\frac{R^2}{(n+2)^2}}\Big)^n, \tag{A.7a}$$

$$s_n^2(R) \,\leq\, b_0 R\Big(n+\frac{1}{2}\Big)^{\frac{2}{3}}\Big(\frac{R^2}{(n+1)^2}e^{1-\frac{R^2}{(n+1)^2}}\Big)^{n+1}, \tag{A.7b}$$

$$t_n^2(R) \,\leq\, b_0\Big(3\sqrt{e}\max\Big\{1, \frac{1}{R}\Big\} + R\Big)\Big(n+\frac{3}{2}\Big)^{\frac{2}{3}}\Big(\frac{R^2}{n^2}e^{1-\frac{R^2}{(n+2)^2}}\Big)^n, \tag{A.7c}$$

where the constant $b_0 \approx 4.791$ is independent of n and R.

Proof. From Lemma A.3 of [8] we find that, for any $n \geq R > 0$,

$$\begin{aligned} s_n^2(R) \,&\leq\, b_0 R\Big(n+\frac{1}{2}\Big)^{\frac{2}{3}}\Big(\frac{R^2}{(n+1)^2}e^{1-\frac{R^2}{(n+1)^2}}\Big)^{n+1} \\ &\leq\, b_0 R\Big(n+\frac{3}{2}\Big)^{\frac{2}{3}}\Big(\frac{R^2}{n^2}e^{1-\frac{R^2}{(n+2)^2}}\Big)^n, \end{aligned} \tag{A.8}$$

where the constant $b_0 \approx 4.791$ is independent of n and R. Furthermore, using Theorem 2 of [16] it can be seen as in the proof of Lemma A.3 of [8] that, for $n \geq R > 0$,

$$\begin{aligned} j_n^2(R) \,&\leq\, \frac{\pi}{2}\frac{2^{\frac{2}{3}}}{3^{\frac{4}{3}}(\Gamma(\frac{2}{3}))^2}\frac{R^{2n}}{(n+\frac{1}{2})^{2n+\frac{5}{3}}}e^{\frac{(n+\frac{1}{2})^2-R^2}{n+1}} \\ &\leq\, \frac{2\pi}{R^2}\frac{2^{\frac{2}{3}}}{3^{\frac{4}{3}}(\Gamma(\frac{2}{3}))^2}\Big(n+\frac{3}{2}\Big)^{\frac{2}{3}}\Big(\frac{R^2}{n^2}e^{1-\frac{R^2}{(n+2)^2}}\Big)^n. \end{aligned} \tag{A.9}$$

Applying the recurrence relation 10.51.2 of [21] shows that

$$|j_n'(R)| \,\leq\, \frac{1}{2}\Big(|j_{n-1}(R)| + \frac{1}{R}|j_n(R)| + |j_{n+1}(R)|\Big)\,,$$

and assuming that $n \geq R > 0$, we obtain from (A.9) that

$$|j_n'(R)| \,\leq\, \frac{3}{2}\max\Big\{1, \frac{1}{R}\Big\}\frac{\sqrt{2\pi}}{R}\frac{2^{\frac{1}{3}}}{3^{\frac{2}{3}}\Gamma(\frac{2}{3})}\Big(n+\frac{3}{2}\Big)^{\frac{1}{3}}\Big(\frac{R^2}{n^2}e^{1-\frac{R^2}{(n+2)^2}}\Big)^{\frac{n}{2}}. \tag{A.10}$$

Combining (A.2) with the estimates (A.8) and (A.10) yields (A.7c). Finally, using (A.9) and (A.7c) gives (A.7a). □

Remark A.5. A bit less explicit but even sharper bounds can be shown using the estimates (9)–(10) on page 255 of [27],[10]

$$J_\nu(r) \,\le\, \frac{e^{-\nu F(\frac{\nu}{r})}}{(1-\frac{r^2}{\nu^2})^{\frac14}\sqrt{2\pi\nu}} \quad\text{and}\quad J_\nu'(r) \,\le\, \frac{\nu}{r}\frac{e^{-\nu F(\frac{\nu}{r})}}{\sqrt{2\pi\nu}}\Big(1+\frac{r^2}{\nu^2}\Big)^{\frac14}, \qquad 0<r\le\nu\,, \quad \text{(A.11)}$$

where

$$F(s) \,=\, \log(1+\sqrt{1-s^2}) - \log(s) - \sqrt{1-s^2} \,=\, \sum_{m=1}^{\infty} \frac{(\sqrt{1-s^2})^{2m+1}}{2m+1}\,, \qquad 0<s\le 1\,,$$

is strictly monotonically decreasing.

Substituting (A.11) into (A.1) and using (A.4) we find that, for $0<R<\nu := n+\frac12$,

$$\begin{aligned} s_n^2(R) \,&\le\, \pi\int_0^R \frac{r}{\nu}\frac{e^{-2\nu F(\frac{r}{\nu})}}{\sqrt{1-\frac{r^2}{\nu^2}}}\,\mathrm{d}r \,\le\, \pi\nu e^{-2\nu F(\frac{R}{\nu})}\int_0^{\frac{R}{\nu}} \frac{t}{\sqrt{1-t^2}}\,\mathrm{d}t \\ &=\, \pi\nu\Big(1-\sqrt{1-\frac{R^2}{\nu^2}}\Big)e^{-2\nu F(\frac{R}{\nu})} \,\le\, \pi\nu e^{-2\nu F(\frac{R}{\nu})}\,. \end{aligned}$$

Furthermore, assuming that $0<R^2\le\nu^2-\frac{1}{\nu}$, i.e., $\frac{1}{\sqrt{\nu^2-R^2}}\le\sqrt{\nu}$, we obtain from (A.11) that

$$4\pi R j_n^2(R) \,=\, 2\pi^2 J_\nu^2(R) \,\le\, 2\pi^2\frac{e^{-2\nu F(\frac{\nu}{R})}}{2\pi\sqrt{\nu^2-R^2}} \,\le\, \pi\sqrt{\nu}e^{-2\nu F(\frac{\nu}{R})}$$

and

$$\begin{aligned} |2\pi R^2(j_n^2)'(R)| \,&=\, |2\pi^2 R J_\nu(R)J_\nu'(R) - \pi^2 J_\nu^2(R)| \\ &\le\, \pi e^{-2\nu F(\frac{\nu}{R})}\frac{(\nu^2+R^2)^{\frac14}}{(\nu^2+R^2)^{\frac14}} + \pi^2\frac{e^{-2\nu F(\frac{\nu}{R})}}{2\pi\sqrt{\nu^2-R^2}} \,\le\, \pi\Big(2^{\frac14}\nu^{\frac34}+\frac12\nu^{\frac12}\Big)e^{-2\nu F(\frac{\nu}{R})}\,. \end{aligned}$$

Accordingly, we have shown that, for $0<R^2\le\nu^2-\frac{1}{\nu}$ and $\nu := n+\frac12$,

$$r_n^2(R) \,=\, \pi\nu(e^{-2F(\frac{R}{\nu})})^\nu\Big(1+2^{\frac14}\nu^{-\frac14}+\frac32\nu^{-\frac12}\Big)\,, \qquad \text{(A.12a)}$$

$$s_n^2(R) \,=\, \pi\nu(e^{-2F(\frac{R}{\nu})})^\nu\,, \qquad \text{(A.12b)}$$

$$t_n^2(R) \,=\, \pi\nu(e^{-2F(\frac{R}{\nu})})^\nu\Big(1+2^{\frac14}\nu^{-\frac14}+\frac12\nu^{-\frac12}\Big)\,. \qquad \text{(A.12c)}$$

This should be compared to (A.7). ◊

When $n<R$, the rescaled squared singular values, $r_n^2(R)$, $s_n^2(R)$, and $t_n^2(R)$, are not small, as can be seen from the following lemma. We denote by $\lceil\nu R\rceil$ is smallest integer that is greater than or equal to νR.

Lemma A.6.

$$\lim_{R\to\infty}\frac{r_{\lceil\nu R\rceil}^2(R)}{2\pi R} \,=\, \lim_{R\to\infty}\frac{s_{\lceil\nu R\rceil}^2(R)}{2\pi R} \,=\, \lim_{R\to\infty}\frac{t_{\lceil\nu R\rceil}^2(R)}{2\pi R} \,=\, \begin{cases} \sqrt{1-\nu^2}\,, & \nu\le 1\,, \\ 0\,, & \nu>1\,. \end{cases}$$

[10] The estimates (A.12) below and their proofs were found by the anonymous referee of this paper.

Proof. Using Landau's estimate (53) and the recurrence relation [21, 10.51.1], we find that, for any $n \in \mathbb{N}$,

$$|j_n^2(R)| \,\leq\, b_1^2 R^{-\frac{5}{3}} \qquad \text{and} \qquad |j_n'(R) j_n(R)| \,\leq\, 2b_1^2 R^{-\frac{5}{3}}\,.$$

Accordingly, using (A.2),

$$\begin{aligned} |t_n^2(R) - s_n^2(R)| \,&=\, 4\pi R^2 |j_n'(R) j_n(R)| \,\leq\, 8\pi b_1^2 R^{\frac{1}{3}}\,, \\ |r_n^2(R) - t_n^2(R)| \,&=\, 4\pi R |j_n^2(R)| \,\leq\, 4\pi b_1^2 R^{\frac{1}{3}}\,. \end{aligned}$$

The result now follows from Corollary A.10 of [8], where we have already shown that

$$\lim_{R\to\infty} \frac{s^2_{\lceil \nu R \rceil}(R)}{2\pi R} \,=\, \begin{cases} \sqrt{1-\nu^2}\,, & \nu \leq 1\,, \\ 0\,, & \nu > 1\,. \end{cases}$$

□

B. Triple products of vector spherical harmonics

Finally, we prove an "orthogonality property" for vector spherical harmonics that we haven't been able to find in the literature.

Lemma B.1. *Let $l, m, n \in \mathbb{N}$, $\alpha_l \in \mathbb{Y}_l$, $\beta_m \in \mathbb{Y}_m$, and $\gamma_n \in \mathbb{Y}_n$. If $l > m + n$ or $l < |m - n|$, then*

$$\int_{S^2} \alpha_l(\boldsymbol{\theta})(\mathbf{Grad}\,\beta_m(\boldsymbol{\theta}) \cdot \mathbf{Grad}\,\gamma_n(\boldsymbol{\theta}))\,\mathrm{d}s(\boldsymbol{\theta}) \,=\, 0\,, \tag{B.1a}$$

$$\int_{S^2} \alpha_l(\boldsymbol{\theta})(\mathbf{Grad}\,\beta_m(\boldsymbol{\theta}) \cdot \mathbf{Curl}\,\gamma_n(\boldsymbol{\theta}))\,\mathrm{d}s(\boldsymbol{\theta}) \,=\, 0\,, \tag{B.1b}$$

$$\int_{S^2} \alpha_l(\boldsymbol{\theta})(\mathbf{Curl}\,\beta_m(\boldsymbol{\theta}) \cdot \mathbf{Curl}\,\gamma_n(\boldsymbol{\theta}))\,\mathrm{d}s(\boldsymbol{\theta}) \,=\, 0\,. \tag{B.1c}$$

Proof. In the following we denote for any $j \in \mathbb{N}$ by $\mathbb{H}_j$ the space of (scalar) homogeneous polynomials of degree j in 3 dimensions, and by $\mathbb{H}_j^3$ the space of three-vectors consisting of homogenous polynomials of degree j in each component.

Given any spherical harmonic $\alpha_n \in \mathbb{Y}_n$, the extension

$$a_n(\boldsymbol{x}) \,:=\, |\boldsymbol{x}|^n \alpha_n(\widehat{\boldsymbol{x}})\,, \qquad \boldsymbol{x} \in \mathbb{R}^3\,, \tag{B.2}$$

belongs to $\mathbb{H}_n$. Accordingly,

$$\nabla a_n(\boldsymbol{x}) \,=\, n|\boldsymbol{x}|^{n-1}\alpha_n(\widehat{\boldsymbol{x}})\widehat{\boldsymbol{x}} + |\boldsymbol{x}|^{n-1}\mathbf{Grad}\,\alpha_n(\widehat{\boldsymbol{x}})\,, \qquad \boldsymbol{x} \in \mathbb{R}^3\,, \tag{B.3}$$

belongs to $\mathbb{H}_{n-1}^3$ and satisfies $\Pi_{\widehat{\boldsymbol{x}}}(\nabla a_n(\widehat{\boldsymbol{x}})) = \mathbf{Grad}\,\alpha_n(\widehat{\boldsymbol{x}})$. Furthermore,

$$\boldsymbol{x} \times \nabla a_n(\boldsymbol{x}) \,=\, -|\boldsymbol{x}|^n \mathbf{Curl}\,\alpha_n(\widehat{\boldsymbol{x}})\,, \qquad \boldsymbol{x} \in \mathbb{R}^3\,, \tag{B.4}$$

belongs to $\mathbb{H}_n^3$ and satisfies $\Pi_{\widehat{\boldsymbol{x}}}(\widehat{\boldsymbol{x}} \times \nabla a(\widehat{\boldsymbol{x}})) = -\mathbf{Curl}\,\alpha_n(\widehat{\boldsymbol{x}})$.

Now let $l, m, n \in \mathbb{N}$, $\alpha_l \in \mathbb{Y}_l$, $\beta_m \in \mathbb{Y}_m$, $\gamma_n \in \mathbb{Y}_n$. Then the extensions $b_m(\boldsymbol{x}) := |\boldsymbol{x}|^m \beta_m(\widehat{\boldsymbol{x}})$ and $c_n(\boldsymbol{x}) := |\boldsymbol{x}|^n \gamma_n(\widehat{\boldsymbol{x}})$, $\boldsymbol{x} \in \mathbb{R}^3$, belong to $\mathbb{H}_m$ and $\mathbb{H}_n$, respectively, and (B.3)–(B.4) show that

$$|\boldsymbol{x}|^2 \nabla b_m(\boldsymbol{x}) \cdot \nabla c_n(\boldsymbol{x}) \;=\; |\boldsymbol{x}|^{m+n} (mn \beta_m(\widehat{\boldsymbol{x}}) \gamma_n(\widehat{\boldsymbol{x}}) + \mathbf{Grad} \beta_m(\widehat{\boldsymbol{x}}) \cdot \mathbf{Grad} \gamma_n(\widehat{\boldsymbol{x}}))\,, \quad x \in \mathbb{R}^3\,,$$

belongs to $\mathbb{H}_{m+n}$, while

$$(\boldsymbol{x} \times \nabla b_m(\boldsymbol{x})) \cdot \nabla c_n(\boldsymbol{x}) \;=\; -|\boldsymbol{x}|^{m+n-1} \mathbf{Curl} \beta_m(\widehat{\boldsymbol{x}}) \cdot \mathbf{Grad} \gamma_n(\widehat{\boldsymbol{x}})\,, \qquad \boldsymbol{x} \in \mathbb{R}^3\,,$$

belongs to $\mathbb{H}_{m+n-1}$. Accordingly, $\mathbf{Grad}\, \beta_m \cdot \mathbf{Grad}\, \gamma_n \;=\; \mathbf{Curl}\, \beta_m \cdot \mathbf{Curl}\, \gamma_n$ extends to $\mathbb{H}_{m+n}$, and that $\mathbf{Grad}\, \beta_m \cdot \mathbf{Curl}\, \gamma_n$ extends to $\mathbb{H}_{m+n-1}$. Since

$$\Big(\sum_{j=0}^{m+n} \mathbb{H}_j\Big)\Big|_{S^2} \;=\; \mathbb{Y}_{\le m+n} \;:=\; \bigoplus_{j=0}^{m+n} \mathbb{Y}_j$$

(cf. [1, Corollary 2.19]), we obtain (B.1) for $l > m+n$, because $\mathbb{Y}_l \perp \mathbb{Y}_{\le m+n}$.

Using integration by parts shows that

$$\begin{aligned}
&\int_{S^2} \alpha_l(\boldsymbol{\theta}) (\mathbf{Grad}\, \beta_m(\boldsymbol{\theta}) \cdot \mathbf{Grad}\, \gamma_n(\boldsymbol{\theta}))\, \mathrm{d}s(\boldsymbol{\theta}) \\
&= -\int_{S^2} (\mathbf{Grad}\, \alpha_l(\boldsymbol{\theta}) \cdot \mathbf{Grad}\, \beta_m(\boldsymbol{\theta})) \gamma_n(\boldsymbol{\theta})\, \mathrm{d}s(\boldsymbol{\theta}) + n(n+1) \int_{S^2} \alpha_l(\boldsymbol{\theta}) \beta_m(\boldsymbol{\theta}) \gamma_n(\boldsymbol{\theta})\, \mathrm{d}s(\boldsymbol{\theta}) \\
&= -\int_{S^2} (\mathbf{Grad}\, \alpha_l(\boldsymbol{\theta}) \cdot \mathbf{Grad}\, \gamma_n(\boldsymbol{\theta})) \beta_m(\boldsymbol{\theta})\, \mathrm{d}s(\boldsymbol{\theta}) + m(m+1) \int_{S^2} \alpha_l(\boldsymbol{\theta}) \beta_m(\boldsymbol{\theta}) \gamma_n(\boldsymbol{\theta})\, \mathrm{d}s(\boldsymbol{\theta})
\end{aligned}$$

and

$$\begin{aligned}
&\int_{S^2} \alpha_l(\boldsymbol{\theta}) (\mathbf{Grad}\, \beta_m(\boldsymbol{\theta}) \cdot \mathbf{Curl}\, \gamma_n(\boldsymbol{\theta}))\, \mathrm{d}s(\boldsymbol{\theta}) \\
&\qquad = -\int_{S^2} \beta_m(\boldsymbol{\theta}) (\mathbf{Grad}\, \alpha_l(\boldsymbol{\theta}) \cdot \mathbf{Curl}\, \gamma_n(\boldsymbol{\theta}))\, \mathrm{d}s(\boldsymbol{\theta}) \\
&\qquad = \int_{S^2} \gamma_n(\boldsymbol{\theta}) (\mathbf{Grad}\, \alpha_l(\boldsymbol{\theta}) \cdot \mathbf{Curl}\, \beta_m(\boldsymbol{\theta}))\, \mathrm{d}s(\boldsymbol{\theta})\,.
\end{aligned}$$

Permuting the roles of l, m and n yields (B.1) for $l < |m-n|$. □

Corollary B.2. *Let $l, m, n \in \mathbb{N}$, $\boldsymbol{A}_m \in \mathbb{T}_m$, and $\boldsymbol{B}_n \in \mathbb{T}_n$. If $l > m+n$ or $l < |m-n|$, then*

$$\int_{S^2} P_l(\widehat{\boldsymbol{c}} \cdot \boldsymbol{\theta}) \boldsymbol{A}_m(\boldsymbol{\theta}) \cdot \boldsymbol{B}_n(\boldsymbol{\theta})\, \mathrm{d}s(\boldsymbol{\theta}) \;=\; 0\,. \tag{B.5}$$

In particular, $\boldsymbol{A}_m \cdot \boldsymbol{B}_n \in \mathbb{Y}_{\le m+n}$.

Proof. Because each vector spherical harmonic is the sum of a surface gradient of one spherical harmonic and the surface curl of another, i.e.

$$\begin{aligned}
\boldsymbol{A}_m \;&=\; \boldsymbol{A}_m^{(s)} + \boldsymbol{A}_m^{(t)} \;=\; \mathbf{Grad}\, \alpha_m^{(s)} + \mathbf{Curl}\, \alpha_m^{(t)} \;\in\; \mathbb{U}_m \oplus \mathbb{V}_m \\
\boldsymbol{B}_n \;&=\; \boldsymbol{B}_n^{(s)} + \boldsymbol{B}_n^{(t)} \;=\; \mathbf{Grad}\, \beta_n^{(s)} + \mathbf{Curl}\, \beta_n^{(t)} \;\in\; \mathbb{U}_n \oplus \mathbb{V}_n
\end{aligned}$$

with some $\alpha_m^{(s)}, \alpha_m^{(t)} \in \mathbb{Y}_m$ and $\beta_n^{(s)}, \beta_n^{(t)} \in \mathbb{Y}_n$, the orthogonality relations in Lemma B.1 show (B.5). □

References

[1] K. Atkinson and W. Han, *Spherical Harmonics and Approximations on the Unit Sphere: An Introduction*, Springer, Heidelberg, 2012.

[2] D. Colton and R. Kress, *Inverse Acoustic and Electromagnetic Scattering Theory*, 3rd ed., Springer, New York, 2013.

[3] D. L. Donoho and P. B. Stark, Uncertainty principles and signal recovery, *SIAM J. Appl. Math.*, 49 (1989), 906–931.

[4] W. Freeden and M. Gutting, *Special Functions of Mathematical (Geo-)Physics*, Birkhäuser/Springer, Basel, 2013.

[5] R. Griesmaier, M. Hanke, and J. Sylvester, Far field splitting for the Helmholtz equation, *SIAM J. Numer. Anal.*, 52 (2014), 343–362.

[6] R. Griesmaier and J. Sylvester, Far field splitting by iteratively reweighted ℓ^1 minimization, *SIAM J. Appl. Math.*, 76 (2016), 705–730.

[7] R. Griesmaier and J. Sylvester, Uncertainty principles for inverse source problems, far field splitting and data completion, *SIAM J. Appl. Math.* 77 (2017), 154–180.

[8] R. Griesmaier and J. Sylvester, Uncertainty principles for three-dimensional inverse source problems, *SIAM J. Appl. Math.*, 77 (2017), 2066–2092.

[9] M. J. Grote, M. Kray, F. Nataf, and F. Assous, Time-dependent wave splitting and source separation, *J. Comput. Phys.*, 330 (2017), 981–996.

[10] H. Haddar, S. Kusiak and J. Sylvester, The convex back-scattering support, *SIAM J. Appl. Math.* 66 (2005), 591–615.

[11] P. Hähner, *On Acoustic, Electromagnetic, and Elastic Scattering Problems in Inhomogeneous Media*, Habilitationsschrift, Göttingen, 1998.

[12] F. Ben Hassen, J. Liu, and R. Potthast, On source analysis by wave splitting with applications in inverse scattering of multiple obstacles, *J. Comput. Math.*, 25 (2007), 266–281.

[13] A. Kirsch, The factorization method for Maxwell's equations, *Inverse Problems* 20 (2004), S117–S134.

[14] A. Kirsch and F. Hettlich, *The Mathematical Theory of Time-Harmonic Maxwell's Equations. Expansion-, Integral-, and Variational Methods.*, Springer, Cham, 2015.

[15] I. Krasikov, Uniform bounds for Bessel functions, *J. Appl. Anal.*, 12 (2006), 83–91.

[16] I. Krasikov, Approximations for the Bessel and Airy functions with an explicit error term, *LMS J. Comput. Math.*, 17 (2014), 209–225.

[17] S. Kusiak and J. Sylvester, The scattering support, *Comm. Pure Appl. Math.*, 56 (2003), 1525–1548.

[18] S. Kusiak and J. Sylvester, The convex scattering support in a background medium, *SIAM J. Math Anal.*, 36 (2005), 1142–1158.

[19] L.J. Landau, Bessel functions: monotonicity and bounds, *J. London Math. Soc. (2)*, 61 (2000), 197–215.

[20] L. Lorch, On Bessel functions of equal order and argument, *Rend. Sem. Mat. Univ. Politec. Torino*, 50 (1992), 209–216.

[21] F.W.J. Olver, D.W. Lozier, R.F. Boisvert, and C.W. Clark, eds., *NIST Handbook of Mathematical Functions*, Cambridge University Press, New York, 2010.

[22] R. Potthast, F. M. Fazi, and P. A. Nelson Source splitting via the point source method, *Inverse Problems*, 26 (2010), 045002.

[23] R. Potthast, J. Sylvester, and S. Kusiak, A "range test" for determining scatterers with unknown physical properties, *Inverse Problems*, 19 (2003), 533–547.

[24] M. Scroggs, T. Betcke, E. Burman, W. Śmigaj, and E. van 't Wout, Software frameworks for integral equations in electromagnetic scattering based on Calderón identities, *Comput. Math. Appl.*, 74 (2017), 2897–2914.

[25] W. Śmigaj, T. Betcke, S. Arridge, J. Phillips and M. Schweiger, Solving boundary

integral problems with BEM++, *ACM Trans. Math. Software*, 41 (2015), 40 pp.
[26] J. Sylvester, Notions of support for far fields, *Inverse Problems*, 22 (2006), 1273–1288.
[27] G.N. Watson, *A Treatise on the Theory of Bessel Functions*, Cambridge University Press, Cambridge, 1944.